BUILDING CRACK DETECTION AND CHARACTERIZATION FROM VHR IMAGERY

EFSTRATIOS KARANTANELLIS

MARCH, 2015

SUPERVISORS:

Dr. Norman Kerle

Dr. Markus Gerke

BUILDING CRACK DETECTION AND CHARACTERIZATION FROM VHR IMAGERY

EFSTRATIOS KARANTANELLIS

Enschede, The Netherlands, March, 2015

Thesis submitted to the Faculty of Geo-Information Science and Earth Observation of the University of Twente in partial fulfilment of the requirements for the degree of Master of Science in Geo-information Science and Earth Observation.

Specialization: Applied Earth Sciences: Natural Hazards and Disaster Risk Management

SUPERVISORS:

Dr. Norman Kerle

Dr. Markus Gerke

GRADUATION PROJECT ASSESSMENT BOARD:

Prof. Dr. V. Jetten (Chair)

Dr. C. Percello

ABSTRACT

The last decades, the occurrence of natural and man-made disasters is increasing significantly worldwide. Those hazardous events have tremendous impact on the society with effects like considerable loss of lives and heavy damage on building infrastructure. The integrity of the infrastructure is mostly evaluated with visual interpretation surveys performed by certified structural experts who have the aim to identify visible damage signs on the exterior part of the structure. In addition, the latter procedure is time consuming and subjective on the experts' perspective. Thus, the elements that are visible after an event as initial signs of structural deterioration are cracks. The current research attempts to develop an image based methodological framework to identify the cracking features and provide reliable information for their geometrical properties such as their area, length and maximum width. The current information will constitute an additional tool for detail damage characterization. Furthermore, the use of Very High Resolution (VHR) sensor to collect the data lead to the implementation of Object Based Image Analysis (OBIA) techniques to solve the problem of damage feature extraction with high accuracy and reliability. In addition with the cracking features, holes on the damaged façade were highlighted due to the fact that those damage elements could constitute initial points for crack propagation. Two products were generated from the imagery and then used as inputs in the OBIA. First, the 2.5D DSM of the damaged facade in order to identify depressions on the elevation model that could constitute potential damage features. Second, the orthorectified image of the damaged façade where the damaged elements can be identified with low brightness values compared with the rest of the background. The OBIA stage was proceeded in the software package eCognition by Trimble. The results suggest that the proposed methodology from the initial step of image acquisition till the OBIA seems promising. From damage areas with "simple" damage pattern the accuracy classification result was high in contrary with problematic areas were the results look pessimistic. These results seem significant interesting for stakeholders and institutions that are looking for efficient damage mapping and monitoring of the infrastructure based on VHR imagery.

ACKNOWLEDGEMENTS

I would like to dedicate this research to my family for giving me the opportunity to fulfil my MSc studies and continually keep me focus and calm during my long trip. Also, a special thanks to all of my friends for giving me the strength to overcome all the difficulties.

In addition, I would like to express my sincere appreciation for my supervisors Norman Kerle and Markus Gerke, for their guidance and experience they have given me along this period. Special thanks to all of the ITC stuff and students for their assistance during my studies.

TABLE OF CONTENTS

LIST OF FIGURES

LIST OF TABLES

1. INTRODUCTION

1.1. Background

Damage identification has long played a fundamental role in various domains in order to detect and assess the structural damage on early stage and proceed to appropriate actions for the maintenance and monitoring of civil infrastructure (Burland, Broms, & De Mello, 1977). In order to characterize the damaged features rapidly after a disaster first their geometrical properties needs to be identified and characterized. Organizations such as BAT (2014) and EEFIT (2014) are responsible for executing the procedure of Structural Damage Assessment (SDA) in order to assess the structural stability and safety. SDA constitutes an essential procedure to evaluate the structural integrity and functionality of infrastructure after a disastrous event. The predominant method that has been used for many years in SDA is visual inspection during ground-based surveys. This type of method provides important structural information for the affected areas but it faces serious drawbacks like subjectivity from the visual inspectors and no rapid response. Thus, for the case that rapid results are required it can be too expensive.

Nowadays, there is need for a more robust, repeatable, image based approach for detailed damage mapping (Kerle & Hoffman, 2013) and characterization. Remote sensing techniques try to solve the issue of robustness and automation but they are not so far that much developed in order to provide a definite benchmark which will replace the in situ assessment that experts do (Lemoine, Corbane, Louvrier, & Kauffmann, 2013). Moreover, on the ground, experts map different aspects like damage or safety depending on the procedure and the rules they will follow. The fact that there is no unique approach makes it more difficult to establish this definite truth benchmark. Organizations like United Nations Institute for Training and Research (UNITAR, 2014) have been using remote sensing information and image-based processing methods to identify damaged areas (Kerle & Hoffman, 2013) and provide a characterization of their geometric properties. The use of Unmanned Aerial Systems (UASs) to acquire Very High Resolution (VHR) images in order to extract significant damage information seems to bridge the gap between the traditional ground surveys and remote sensing techniques. Hence, it is less error prone and cost effective compared with the traditional ground-based methods. (Nonami, Kendoul, Suzuki, Wang, & Nakazawa, 2010)

1.1.1. The role of remote sensing in damage assessment

Remote sensing has contributed a lot to the development of damage mapping. However, it is since the last decade that it has been proved as a reliable tool for damage assessment after natural or man-made disasters. An example is the case of Dell'Acqua & Gamba (2012), who presented a holistic review of various remote sensing techniques to evaluate earthquake related damage. Many other scientists have performed a large number of experiments based on change detection techniques on pre- and post-imagery to identify damaged areas after a disaster. A large number of space-borne platforms were used to collect imagery to proceed to SDA. Specifically, Zhang & Kerle (2008) demonstrate a detailed review of the available space-borne sensors for damage assessment procedures. They pointed out the potential limitations such as that the data acquisition after an event is weather dependent (cloud cover). Radar and optical datasets were examined with pre- and post-event datasets while change detection techniques were applied on the imagery. In addition, Tian & Zhang, (2004) applied pre-processing methods such as edge enhancement and change detection techniques on different datasets, from SPOT and airborne images to

SAR images in order to identify damaged areas. Also, Kerle (2010) in his paper presented an underestimation of the structural damage in terms of damage severity and spatial extent in the damage maps that have been produced by UNITAR after an earthquake event in Indonesia.

As the need for more detailed information is unavoidable for the specialists to evaluate the disaster and its consequences, the need for higher spatial resolution is significant. Nowadays, the spatial resolution has been increased up to the level of mm and that gives further possibilities for more efficient solutions.

1.1.2. Building damage assessment

In order to execute a comprehensive per building damage assessment, information for the roof and the facades is needed, as it is stated in Galarreta (2014). Most of the conventional sensors are capturing imagery close to nadir perspective that makes it difficult to collect damage information after an event, related with the building facades. In the early 2000s when Pictometry was founded a solution to this drawback could has been given by the use of the images that this new system could acquire (EagleView, 2014). The latter offers aerial image acquisition from five different viewing directions, simultaneously. One image close to nadir perspective and four oblique images at 40^{o} viewing angle which makes the current method efficient for reliable building damage assessment (Gerke & Kerle (2011), Saito & Spence (2010)). Nowadays, large firms like TNO are looking to develop an image-based framework capable to lead to a detailed characterization of the visible damage signs on façade level. This will enable cost effective solutions as the structural experts will be able to inspect the infrastructure from a safe distance and rapidly.

As mentioned above, the spatial resolution is increasing tremendously with data acquired from new sensors and new airborne platforms that have been introduced with the pace of time. Today, the so-called Unmanned Aerial Vehicles (UAVs) or drones, such as the one from Aibotix (2014), (Figure 1), are capable of hovering over sites and collect imagery that will be used for several purposes. Disastrous sites can be one of these cases that images are captured for damage assessment which usually is conducted by surveyors. These platforms are capable to combine advantages of close range photogrammetry with airborne acquisition. For instance, they can perform low altitude flights and even hover over a predefined location and collect imagery simultaneously. The small height in combination with VHR sensor mounted on the platform constitutes them efficient for post-disaster damage assessments cases. For instance, they are able to capture imagery with cracks less than 1cm in width with the VHR sensors mounted (Chen, Rice, Boyle & Hauser, 2011). However, a serious limitation of UAVs is that they can cover small areas due to the limited flight time. Nowadays, both in private and public sector UAVs are used increasingly for infrastructure monitoring that many times includes building inspection (e.g. SKEYE BV, (2014)).

Figure 1. Aibotix X6 UAV (aibotix.com) (left). UAV performing building inspection (flyrobotimages.de) (right).

1.1.3. From pixel towards object

Since the first days of remote sensing, the traditional way for information extraction was based completely on a pixel level. The last two decades the evolution of remote sensing and close range photogrammetry, with the Very High Resolution (VHR) imagery, has given much more possibilities for analysis. Object-Based Image Analysis (OBIA) that will be used in the current thesis is an approach that takes advantage of the information that can be extracted from these VHR images. Today both terms Object Based Image Analysis (OBIA) and Object Oriented Analysis (OOA) are used but for this thesis the term OBIA has been adopted. The main task of image analysis is to extract real word objects based on some parameters which pixel based approaches are not able to do (Trimble, 2014b). As the spatial resolution is becoming higher, the pixel size is decreasing and the objects are represented better by clusters of pixels (T. Blaschke, 2010).

The traditional pixel-based methods for information extraction are not so reliable to be applied on VHR imagery (Joshi, 2010). Many researchers such as Yamazaki, Suzuki, & Maruyama, (2008), Blaschke & Strobl, (2001) and Haiyang, Gang, & Xiaosan, (2010) have agreed on the reliability of object based image analysis techniques on VHR imagery and they have pointed out that the latter can many times provide more accurate and reliable results than the pixel based approach. Another asset of OBIA is that it can combine spatial, spectral and contextual information of the image to extract the features of interest, while the pixel approach is based on the reflectance statistics of the pixel.

Two are the major stages of OBIA; the first is the segmentation of the imagery into homogenous areas based on a variety of different segmentation algorithms. The second is the classification where the segmented objects, from the previous step, are assigned into meaningful classes based on a set of attributes. Today, these two stages can be repetitively combined such as a case of segmentation - classification - re segmentation – classification, in different object hierarchies.

1.2. Problem statement

The use of VHR optical sensors together with terrestrial and/or airborne platforms can be used for the detailed identification and characterization of damaged features. Holes and cracks on building facades are such damage features and constitute the two classes that will be extracted from imagery on this thesis. Cracks constitute the initial visible signs on the exterior surface of the infrastructure after a hazardous event (FEMA 307, 1998). Thus, they can pose serious deterioration of structural integrity if no restoration actions will be taken in short time from their presence. Currently, there is no methodology based on OBIA techniques that automatically can detect cracks and simultaneously retrieve their properties.

Motivated from the previous, the current study aims to develop an approach for crack identification on façade level, for the cases that the wall has not collapsed after the disaster, by using VHR images and image-based DSM for OBIA. A terrestrial platform with a VHR sensor (Table 3) will be used for the image acquisition of the damaged facades. These facades will be selected based on their constructing material in order to assess the proposed method for each case. Two different illumination conditions will be simulated for the image acquisition, a) with flash light and b) only with ambient lightning. This approach aims to prove if the light enhancement can produce more detailed results.

After the acquisition stage DSM and orthorectified images will be generated and OBIA procedure will follow. First, a hybrid approach will run for the segmentation process by using the DSM in combination with the orthorectified image in order to segment the imagery based on the elevation and colour of the façade's features. Next, the segmented objects will be classified as damage features (holes or cracks) or as background (façade objects) based on a set of properties such as the ratio length/width of the object.

1.3. Research objectives

The objective of this research study is to explore the issues of damage features on facades and develop an image-based framework that can be used for accurate and reliable assessment of surface cracking features. The outcome will be information of the geometrical properties of the crack. The proposed approach aims to enhance the robustness of structural damage assessment procedure. To achieve the objective the following "sub-objectives" which constitute parts of the research study have to be conducted:

1. Develop an approach to automatically identify cracks that constitute damage features on the façade.
2. Create a comprehensive theoretical inventory of the various types of cracks.
3. Design an image acquisition framework to collect imagery from existing cracking features.
4. Demonstrate the use of image-based Digital Surface Model (DSM) and orthophoto information to augment crack characterization.
5. Use of active illumination source to enhance the crack detection and characterization performance from images. Imagery with and without additional illumination will be available for further analysis.
6. Identify and extract the damage features of interest from the overlapping imagery, for both cases, with and without additional illumination source.
7. Characterize the damage features based on their geometric properties (width, length, depth).

1.4. Research questions

1. What are the crack related categories that already have been studied?
2. What are the "to be produced" data from the acquired imagery in order to identify the features of interest?
3. How to segment the images in order to extract accurately the damage features of interest from the sample areas?
4. What are the most important crack's geometrical properties and which of them can be extracted by using image-based techniques?
5. Which information can be used to extract the features of interest by OBIA?
6. Can additional active illumination source enhance the crack result?
7. What is the geometric accuracy of the extracted features characteristics?

1.5. Thesis structure

The current thesis consists of six major chapters and the content of each is given below in details:

Chapter 1: Introduction. The first chapter includes a background description on the methods used in the current thesis. Next, the research problem is outlined followed by the research objectives & questions.

Chapter 2: Literature review. The second chapter provides an extended analysis of the cracking features followed by background related information on existing crack detection methods.

Chapter 3: Methodology. An overview of the methods developed and implemented under the current research is presented in Chapter 3.

Chapter 4: Results. The outcome of the proposed methodology in the current research is presented in this chapter.

Chapter 5: Discussion. The current chapter includes an extended discussion of the results from all phases of the research.

Chapter 6: Conclusion and recommendations. The final chapter gives an overview on the thesis and summarizes the research findings. In addition, conclusions and suggestions for further research are provided in the current chapter. First, a brief sum up of the proposed research and the answers to the proposed research questions are demonstrated. Moreover, future recommendations are highlighted.

2. LITERATURE REVIEW

2.1. Introduction

From the objectives it is clear that the damage features of interest for this study are the crack and the holes which can be an initial sign of deterioration on the infrastructure. In the current research study three different materials are investigated. Nowadays, concrete and brick constitute the mostly used materials for building constructions. Thus, they were selected as representative for this study. The third material that was under the study scope is an insulating material that is usually used in reinforced masonry between the external brick part and the inner concrete part, to prevent the penetration of moisture. This material was selected for our study as it was located in ITC Faculty building that was easily accessible and Terrestrial Laser Scanner data could have been acquired to allow further analysis at the quality assessment step. Under this chapter, a detailed review of the existing surface cracking features will be presented along with a real case scenario of crack damage monitoring. In addition, cases of crack detection and characterization will be presented in the various domains such as civil infrastructure monitoring.

2.2. Surface damage features on buildings

In the building maintenance domain, there are various approaches to identify, characterize, classify in terms of severity and map the surface defects that the current study deals with.

It should also be mentioned that the two distinct terms of safety and damage of a building are different but usually confused. Safety refers to how feasible is for the inhabitants to enter the building after an event. According to the field manual, for post-earthquake safety evaluation of the infrastructure (Applied Technology Council, 2005) the absence of visible deterioration signs classify the building in the highest level of safety. According to the European Macroseismic Scale of 1998 (EMS, 1998), the absence of visible signs of damage classify the building to the lowest damage level. The focus of this thesis is mostly on the damage part rather than on the safety. This is because the results of the damage feature analysis can be afterwards used for safety assessment.

The damaged features on building facades can be distinguished in two categories as minor or major defects, in terms of severity of the structural integrity:

- Visual appearance or aesthetic/cosmetic,
- Serviceability/function or Stability

Visual or aesthetic defects are defined appearances or imperfections on the building structure that do not affect its structural integrity in terms of functionality and stability. In contrast, defects that pose risk in the structural integrity are more severe and they need direct repair otherwise they may lead to structural failure or even complete building collapse. For instance, parameters of damage classification could be the type of damage, the cause or its severity (Georgiou, 2010).

Nowadays, there is no unique approach for mapping the damage and for assessing the severity of the damage. Different authors have suggested different approaches for the classification of the cracks based on their severity. Some of them base the result on the geometrical properties of the crack like width, length and depth and others consider additional information like the spacing of the cracks and their orientation (Figure 2). Usually, this information is collected manually by building inspectors after visual interpretation in situ. This assessment of the structure integrity takes place hours to days after the disaster. According to the Applied Technology Council, (2005) (ATC) the building damage evaluation methods can be done in three distinct steps.

- The first step is a rapid evaluation of the affected area by building inspectors and/or architects. The objective is to quickly evaluate the constructions and categorize them as unsafe or safe. Buildings with moderate damage are proceeding to the next step.
- The second step is a more detailed evaluation of the infrastructure by specialized structural engineers. In this step, manual measurements of the length and width of the damage features are collected for further analysis and essential facilities are being inspected.
- The last step is conducted by civil engineers and is related to detailed engineering investigation of seriously damaged buildings in order to assess the stability and propose possible repairs.

Authors - Institution	Information
Marshall (Worthing & Heath, 2009)	**Length** – Start and finishing point **Width** – Variation along its length **Element** - Structural element that is affected **Location** - Location of crack **Depth** – Partial or full thickness of the wall **Pattern** – Vertical, horizontal, diagonal or stepped
FEMA (306; 307, 1998)	The **width** of individuals cracks The **orientati**on of cracks The number (**density**) of cracks The **spacing** of cracks The **relative size** of crack widths

Figure 2. Damage assessment criteria of cracks.

Another study done by Galarreta, (2014) presents a semi-automated approach that is possible to label the severity of the damaged building based on OBIA techniques. This work is focused on the damage on a building level and does not provide any detailed information on the geometrical properties of the damage features per facade. This is what the current research study will focus on and is later presented in details in chapter 3.

In this research study, the two initials steps in damage evaluation of ATC would be merged and executed by using terrestrial or/and airborne platforms with high resolution sensor mounted on them. This will allow a detailed characterization of the identified damage targeting solely on the cracking features. The proposed methodology will provide additional information that could augment the damage assessment results in terms of severity.

2.2.1. Crack

A cracking feature is defined as a complete or incomplete separation of an object or material into two or more pieces under the action of stresses which exceed the capacity of the study material (ACI 224, (2007) and Santhi, Krishnamurthy, Siddharth, & Ramakrishnan, (2012)). It should be highlighted that usually, most of the buildings after their construction include cracks on them. The latter are cosmetic appearances due to moisture and thermal movements (Holland, 2012). Cracks that pose critical danger for the structural stability are usually due to foundation issues. Figure 3 could be a helpful tool in order to evaluate the cracking features in relation with the severity of the movement. The mentioned table from Burland was created in 1977 and it is widely used as reference in the visual interpretation of the damage from the structural inspectors in order to produce a rapid qualitative damage assessment in a post-event situation.

The major geometrical properties of the cracking features that are examined during the SDA procedure in ground surveys are the width along the crack region and its length (Figure 2). It has to be mentioned that the constructing material in another parameter that plays a vital role in the SDA procedure but the table above presents solely the geometric criteria based on which the latter is done. For example, different damage propagation can be found in the concrete facades and different in the brick material as the tensile strength of the materials is different. Even if the propagation is different among the various materials, the potential damage features (cracks) that can be found on them can be similar. The location of the damage feature can indicate if a structural element like a pillar is crossed from a damage feature and pose danger in the building stability. Consequently, the relative position of the crack on the entire building construction is another parameter that can contribute in the severity of the damage feature. In addition, the depth of the crack is additional information in order to assess the damage of the façade. In ground surveys, the inspectors usually use a thin ruler inside the crack area to measure the depth until the it stops. Again the depth acquisition is subjective because the variation along the crack region could be high. As a result the, the surveyor is measuring in multiple areas of the crack to estimate a statistically strong measurement of the depth. An alternative method to characterize cracking features is their respective orientation in relation with the geometry of the façade. This information is vital in order to understand the source of cracking by exploiting the pattern and the direction.

More specific, based on their respective properties such as orientation and width, cracking features can be further sorted in the following categories:

1. Based on the orientation cracks can be sorted as:
    - **Horizontal**: cracks which are parallel to the longitudinal axis of the building
    - **Vertical**: cracks which are vertical to the longitudinal axis of the building
    - **Diagonal**: cracks with angle 45^0 approximately to the longitudinal axis of the building

2. Crack Width – Damage Level (Figure 3)

Description	Width	Severity
Hairline cracks, negligible	<0.1mm	Negligible
Fine cracks, rarely visible, damage to internal walls	0.1mm – 1mm	Very slight
Cracks easily filled	1mm – 5mm	Slight
Doors and windows sticking (wide cracks)	5mm – 15mm	Moderate
Windows and door frames distorted, loss of bearing in beams	15mm – 25mm	Severe
Danger of instability – major repair job	>25mm	Very severe

Figure 3. Relation Crack Width vs Damage Level (adapted by Burland et al., (1977))

2.2.2. Main reason of cracking

In general, the wall cracking causes can be distinguished in two major categories, a) the cracking features that result from external loads (structural cracks) and b) those from non-load issue (Non-structural cracks) (Temperature, shrinkage, shearing). (Kashyzadeh & Kesheh, 2012) To distinguish the actual cause of cracking is not always an easy task in the field of structural monitoring and usually it can be really time consuming.

The first category of external loads refers to the issue of natural hazards such as earthquake and landslide or to man-made hazards such as terrorist attacks. After those hazardous events the first visible signs of deformation on the concrete and masonry wall structures are the cracking features, (FEMA 307, 1998).

The second category refers to construction distresses that come off due to climate, poor mixture or constructing variables, ageing of the structure integrity, poor workmanship etc. Usually, the non-structural cracks are damage features that do not affect the stability of the structure.

Every country has different distinct levels that they distinguish between harmful and harmless cracks. As seen in Figure 4 there is not a common threshold of harmful crack width. This makes it difficult to establish a common methodology to define if a crack poses danger on the building integrity by examining solely the size. A reason for this issue could be that each country implements different structural/constructing methods and as a result the structural damage assessments are based on the individual countries' practices. From Figure 4 it is clear that the values which are considered as important crack widths are difficult to become identifiable by an image based analysis. For the current study the mean GSD of the images is from 3mm to 5mm which means that all the objects of smaller dimensions cannot be visible on the images. Thus, no crack features smaller than the GSD value could be mapped.

Institute	Crack width
American Regulation (ACL 224)	0.108 mm
France Regulation (CCBA)	0.27 mm
Canadian Regulation	0.064 mm
Poland Regulation	0.182 mm

Figure 4. Width thresholds of harmful crack (Li, 2012)

2.2.3. Crack growth stages

There are three general distinct growth stages in the cracking procedure (Sabnavis, Kirk, Kasarda, & Quinn, 2004). The first stage (Figure 5a) includes small hairline discontinuities that are initiating on the material without posing any direct danger on structural stability. Cracks of that type have a width value usually less than 0.5cm.

In the second stage (Figure 5b) the crack size is growing significantly. The width is exceeding 1cm and the crack has a substantial depth which needs restoration in order to maintain the building and prevent further damage that may affect the building integrity. The authors Bloch & Geitner, (2012) pointed out that there is a strong relation between the width and the depth growth.

The last stage (Figure 5c) of the cracking procedure is the failure of the material (wall) due to external forces or loads. The latter stage occurs rapidly, after the crack reaches a critical size as a result the material (Brittle or ductile) is not able to withstand the applied forces and it fails.

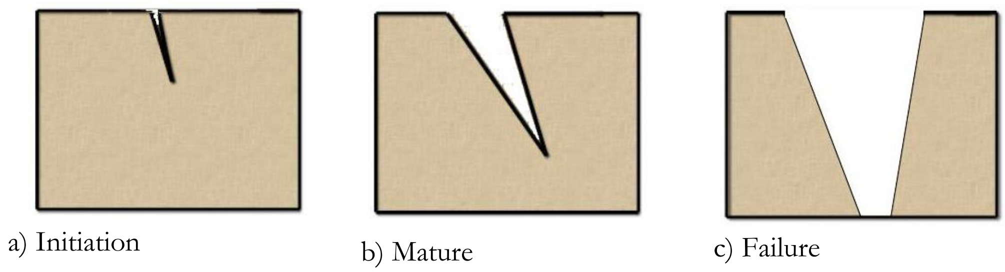

Figure 5. Stages of crack growth (based on (Sabnavis et al., 2004))

2.3. Real case scenario

Under this section a real case scenario of building damage assessment in Groningen will be presented. This case constitutes a semi-automated SDA approach. The subsurface of Netherlands contains several gas and oil fields reservoirs (Figure 6). The majority of these hydrocarbon reservoirs are situated on the north part of the Netherlands. More specific, in the wide area of Groningen there is one of the largest gas fields in the world and probably the largest in the Western Europe. As a result from 1963, there is significant gas production from Groningen field in order to profit the whole country and even for exporting to other countries.

The company responsible for the gas production is NAM (Nederlandse Aardolie Maatschappij BV) based in Netherlands with expertise in oil and gas production. However, the last years there is an upward trend of earthquake events in the wide area of Groningen due to gas extraction and many people have started to worry about their properties and their living environment.

According to scientists working in the area, these tremors have been caused completely by the gas extraction, known as induced earthquakes in the north part on Netherlands. In order to understand the situation of earthquake-induced structural damage a detailed explanation is provided below. First, during the gas production the pore pressure in the sediments is decreasing rapidly. As a result, the area faces serious problems of subsidence. This issue has been brought up several structural problems to the habitants of the wide area of Groningen. Many residential buildings, public infrastructure and monuments have showed serious signs of deterioration due to the effect of subsidence that in some areas like Loppersum can reach 2-6cm in z-axis per year. As a result, cracks are the initial signs of deterioration that are visible on the infrastructure during the monitoring process. Nowadays, the experts are trying to develop information based on structural observations and design documentation strategy for the following years in order to meet the structural requirements under the new problematic situation.

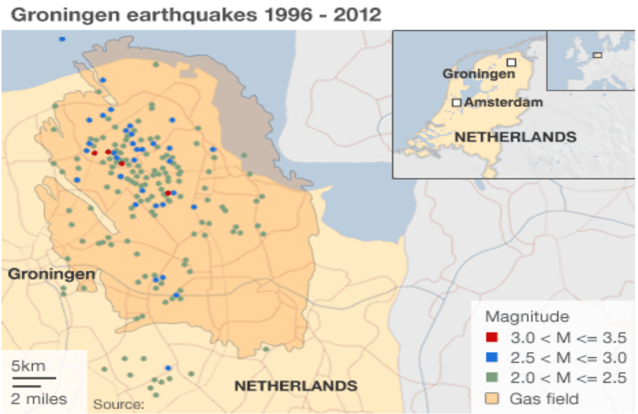

Figure 6. Groningen gas field (www.bbc.co.uk)

TNO or Netherlands Organisation for Applied Scientific Research is a non-profit organization based in Netherlands with expertise on applied science. Moreover, they are responsible for the building damage assessment in Groningen area and provide consultation on structural upgrading of the current infrastructure. After a field visit at TNO's offices and a fruitful discussion with Mr. Marc Hamburg, senior project manager and Mr. Huibert Borsje, senior scientist in the area of Groningen a lot of information were collected in order to relate the current MSc research with the procedures of TNO's SDA approach. In order to execute the structural damage assessment, TNO experts have divided the methodology in three stages (Figure 7).

Firstly, TNO specialists had installed 200 sensors (ground accelerometers) on the edge of buildings with the terrain, around Groningen (50km radius from city center) to measure the dynamic impact of the induced tremors on the buildings. For instance, Loppersum which is one of the high risk areas, 83 buildings are monitored on a daily basis by measuring the Peak Ground Acceleration (PGA).

At the same time, a camera captures a single snapshot of the building façade in order to assess the change or growth of the damage. The camera is activated based on predefined vibration threshold of 1mm/second. For example, the camera will collect an image sample of the façade if the accelometer in the current building exceeds the mentioned PGA threshold.

In addition, the experts are implementing image analysis techniques such as change detection on individual imagery between time intervals to assess the presence or growth of the cracking features. Their method is based completely on qualitative analysis of the presence/absence of cracking features and a quantitative part is missing in order to derive adequate crack information.

The last step in SDA by TNO contains a field visit from structural engineers and specialist to assess the structural damage in situ and provide recommendation for the visible damages. The building assessment by the structural experts is mainly based on assessment of the visible cracking features after an event. This is done by measuring the total length of the visible part of the crack on the façade and relates the damage with one of the 9 building categories that TNO experts defined based on a set of variables such as the age of the building, the structural material and the number of floors. Thus, in terms of visibility of cracking elements, TNO defines theoretically as the least crack entity a hairline crack of 0.5cm. Next, they proceed with a correlation of the magnitude of the tremor in relation with the visible damages.

The result of the above correlation is a first step to categorize the building in one of the EMS-98 damage scales. The latter constitutes the most wide used scale for post disaster damage mapping. Nowadays, the majority of the damaged infrastructure in Groningen is categorized among the 1^{st}, 2^{nd} or 3^{rd} grade of the EMS scale according to the experts. This means that most of the buildings show from slight to moderate damage with hairline to wide cracks on walls and partial collapse of small pieces of plaster.

The outcome of the current methodology which is applied in Groningen area is to produce a statistical analysis of the produced damages from induced earthquakes in order to understand and enhance the structural plan for the following years in Groningen. The current damage assessment approach by TNO could be enhanced by the integration of the proposed workflow of this research. The stage of image acquisition and damage identification could be augmented with the use of the DSM and the orthophoto of the damaged façade. In order to test the applicability of the current approach, experiments have to take place after an event in order to check the quality of the results.

Figure 7. TNO's monitoring approach for damage monitoring in Groningen

2.4. Crack detection methods

In previous sections all possible types of cracks have been explained and illustrated. Also, the growing stages and several ways for crack classification. In the current section the applied crack detection methods will be presented.

In the last two decades, many attempts have been made to detect and identify cracking features and elongated fissures on various materials based on image analysis techniques in a variety of different disciplines (infrastructure maintenance, civil engineering, geology and cultural heritage). Each of these applications has a distinct accuracy level.

Nowadays, in the field of infrastructure monitoring and inspection, an extensive body of literature exists. In the domain of bridge monitoring, Abudayyeh, Al Bataineh, & Abdel-Qader, (2004) demonstrate a general image-based framework for automated bridge inspection. The study presents a holistic pipeline to proceed in bridge assessment. Next, Metni and Hamel (2007) used Unmanned Aerial System (UAS) to acquire imagery in order to monitor and assess damage on bridge decks by identifying cracking features.

More specific, they implemented techniques to optimize the camera's field of view solely on the area of interest. In the same field, Adhikari, Moselhi and Bagchi, (2014) developed a methodology based on multi-temporal image comparison of cracks' length and width on bridges to assess the degree of deterioration based on change detection techniques. Moreover, Abdel-Qader, Abudayyeh, & Kelly, (2003), provide a complete review of four edge detection algorithms. They compared Canny, Fourier and fast Haar transform and Sobel algorithm and they concluded that fast Haar transform had the best results on crack detection on concrete bridges. In addition, Abdel-Qader, Pashaie-Rad, Abudayyeh and Yehia, (2006) proposed a new approach for identifying cracks on concrete bridges by following statistical approach and more specific, Principal Component Analysis (PCA) based techniques. Oh et al. (2009) suggested the use of a robotic inspector system to automatically capture images of bridge decks and detect crack lines based on tracing algorithms. In the last years, Li (2013) proposed a modified image processing method to identify and measure the width of the cracks on bridge decks with millimetre accuracy. They, perform a comparison analysis of the proposed method with edge detection and morphology operators.

In the early 1990's, Tsao, Kehtarnavaz, Chan and Lytton, (1994) proposed an new image approach to assess pavement for potential damage and more specific for cracking fissures. They implemented image analysis techniques to automatically detect cracks on pavements without any manual interaction. Santhi et al., (2012) implemented the canny edge detection operator on grey converted images to automatically identify cracks on pavements. They assumed that the cracks have darker regions on the images in contrast with the rest of the background. Amarasiri, Gunaratne, & Sarkar, (2010) developed a methodology to model crack depth in relation with their respective width on concrete pavements. They based their assumptions on different spectral reflectance of the discontinuities which represent the cracked areas.

Later, Iyer and Sinha, (2005) followed mathematical morphology operators to produce a binary "crack map" to calculate the crack's properties in order to evaluate the condition of underground sewer pipelines. Yu, Jang, & Han, (2007) proposed an automatic inspection system using a robot to detect cracks in low lighting conditions in tunnels. The robot was collecting images from a constant distance and a crack recognition step was following with identification of their respective width, length and location. Liu, Suandi, Ohashi, & Ejima, (2002) proposed an image-based crack detection and classification method incorporating Support Vector Machines (SVM) to distinguish damage in three categories. Recently, a European Commission project called ROBINSPECT (FP7) started to be developed by a collaboration of companies. Based on that, a robotic system will automatically detect and measure deformations inside tunnels and provide an accurate evaluation of the infrastructure. Different methods will be implemented such as image analysis techniques from very high resolution cameras to vibration propagation analysis. In addition, active illumination will be used in order to enhance the lightning conditions inside the tunnel.

In civil engineering domain, and specifically in the construction monitoring and maintenance, Niemeier, Riedel, Fraser, and Neuss, (2008) implemented a new digital semi-automated crack monitoring system for calculating the width of cracks in concrete structures. They used the so-called Digital Crack Monitoring System (Digitales Rissmess System – DRS), which was developed by civil and geodetic engineers in Germany. Also, Yamaguchi and Hashimoto, (2009) developed a workflow based on the percolation model to identify cracks' connectivity among neighbouring pixels in the image and edge detection algorithms to detect them on large size concrete surfaces. Moreover, Zhu, German and Brilakis, (2011) proposed a workflow to identify cracks using edge detection and linear percolation on concrete surfaces in a post-disaster situation and retrieve crack properties (orientation, length, width) based on image thinning and distance transformation. Sohn & Lim, (2005) pinpoints a crack monitoring system for concrete structures. They used multitemporal images to estimate the changes of crack width and length by implementing image processing techniques such as image enhancement and histogram thresholding. In addition, Chen, Shao, Jan, Huang, & Tien, (2006) proposed a semiautomatic method based on multitemporal images to measure cracks on images. The results proved that even cracks of 0.05 mm in width could be recognized successfully.

Furthermore, Martins, Junior Pizolato, & Belini, (2013)developed a mobile vision system to inspect crack opening on concrete and masonry. They implemented image processing techniques to automatically identify the width of the cracks by measuring the number of pixels in the cracked region. Valença, Dias-da-Costa, & Júlio, (2012) suggested an automatic crack monitoring system based on photogrammetry and image processing techniques. They performed a laboratory loading test on a concrete specimen while they were collecting images in order to monitor the cracks in different stages of their evolution until the complete structure failure. On the other hand Jahanshahi and Masri, (2012) introduced an image-based workflow based on 3D scene reconstruction, image processing techniques and pattern recognition in order to identify cracks by incorporating Unmanned Aerial Vehicle (UAV). Torok, Fard, & Kochersberger, (2012) and later Torok, Golparvar-Fard, & Kochersberger, (2014) attempted to detect cracks by reconstructing the 3D model of the scene. They used a mini-robot to capture multiple images around a damaged concrete column to illustrate the procedure in a post-disaster situation. Next, the 3D model of the column was created and an algorithm based on the angle of the surface was identifying if the element was a cracked or not cracked region. Last year a novel EU project named RECONASS started to be established. Its objective is to design a series of remote sensing techniques to monitor critical concrete facilities in earthquake prone areas.

Lately, in the field of Geology, Stumpf, Malet, Kerle, Niethammer and Rothmund, (2013) attempted to identify surface fissures in an active slow moving landslide using multi-temporal data and Object Based Image Analysis (OBIA) techniques. Also, Riquelme and Abellán, (2014) used 3D LiDaR data from a Terrestrial Laser Scanner (TLS) to identify rock slope discontinuities based on local curvature and statistical analysis of the plane poles in order to assess the rock slope stability in Spain.

In the field of cultural heritage, the work is limited but the main focus is on virtual restoration of crack on paintings. For instance, Giakoumis, Nikolaidis, and Pitas, (2006) puts forward a new methodology to identify cracks on digitized paintings; they defined a threshold on the result of the top-hat transform. Their assumption was based on the concept that cracks have low luminance and elongated structural characteristics.

Besides image-based crack detection methods, a number of researchers attempted to identify cracks on infrastructure with various methods such as ultrasound waves or vibration techniques in order to identify the cracking features and produce a quantitative analysis.

In the early 1990's the laser scanner made the first steps in the field of structural damage monitoring (Fritsch & Kilian, 1994). Moreover, Arias and Achenbach, (2004) developed a model based on a scanning laser source to detect cracks by generating ultrasound waves. He used the produced echoes from the incident and scattered fields to identify surface-breaking cracks on the surface. Consequently, the laser technology constitutes a reliable solution to provide a detailed 3D model of the crack region.

Ohno & Ohtsu, (2010) proposed a methodology based on acoustic emission to classify the cracks on concrete surfaces in three distinct classes based on their respective frequencies. The same method was followed by Keshtgar & Modarres, (2013). On the other hand, Asnaashari & Sinha, (2014) proposed a framework for crack detection based on vibration responses of tested structure.

From the previous it is clear that many scientists have tried to establish an approach on the crack detection, characterization and severity assessment. However, as already has been mentioned there is no unique methodology for automatic damage feature extraction based on OBIA techniques and for most of the cases this extraction today is done manually (in situ measurements) or semi-manually (e.g. Groningen). Consequently, there is need for an approach which will focus on OBIA techniques when VHR imagery and image based DSM will be used as input data. This will lead to identification and extraction of the damage features per building facade. From the last statement, it is clear that the surface unit in the current thesis will be the façade. The output of this procedure is expected to give at least the width and length of the crack that have been identified as two of the major properties. If this will be achieved then the crack extraction from building facades can be more automated, efficient and cost effective for the stakeholders. This information can also contribute to the development of the current semi-automated approaches.

Concrete material			SEVERITY	Brick material		
Hairline cracks	Shallow cracks width<0.1mm	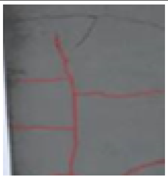	simple	**Broken bricks - aesthetic cracks**	Small shallow cracks on brick surface	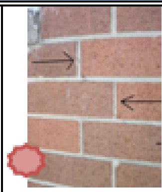
Crazing	Network pattern of fine cracks that do not penetrate below the surface	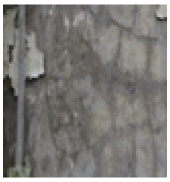		**Brick spalling - holes**	Circular or oval depressions on surface, depends on the structure	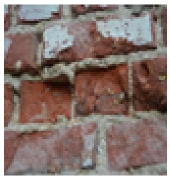
continuous cracks	Elongated cracking features, width vary from 1mm to more than 25mm			**Single continuous cracks**	Elongated cracking features, usually across the weak joints	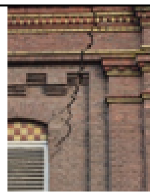
Delamination - Holes	Circular or oval depressions on surface (3mm-25mm)			**Stair-stepped cracks**	Crack pattern across the mortar joints or bricks	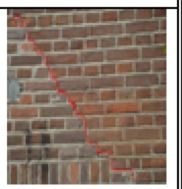
www.stonehengemasonry.ca www.foundationspecialties.com			complex	**Wall displacement**	Horizontal movement across the mortar joints	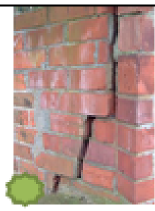

Table 1. Damage Index

After careful literature review and extensive discussions with structural experts Table 1 was created which illustrates the damage features that are related with the cracks on the two mostly used constructing materials, brick and concrete. The damage index constitutes an initial reference of the crack damages that have been come across during the experiments in the current thesis. The sequence of the damage features is sorted from simple cases to more complex ones.

3. METHODOLOGY

Under this sector the proposed methodological approach of the current study will be presented. From the literature review it is clear that today the technological developments give many possibilities for automated ways of damage feature extraction and classification in terms of severity. However, only semi-automated ways have been adapted so far. Here the proposed approach will take advantage of the information that can be extracted from very high resolution images via OBIA techniques in order to extract geometrical properties of these features that can further be used for assessment in terms of severity.

For assessing the severity of damage, information about its geometrical properties need to be known. The damage features here are a) the cracks and b) the holes and the "surface unit" is part of the building façade without other structural elements like windows and doors. If the geometric properties of the damage are known per façade then this information can be composed for making conclusions for the damage severity per building. Thus, the focus is on how to characterize the damage features per façade and not on how to assess them in terms of severity. The flowchart of the current methodology is briefly illustrated in Figure 9.

The first step was the site selection. For a real case scenario the site will be located were the disastrous event will happen but for this study already damaged buildings were found in order to simulate the disaster site. After that the image acquisition was done using a terrestrial platform and a VHR sensor (Figure 8)

These images will be used for photogrammetric analysis. Consequently, there was need to establish an arbitrary local coordinate reference system on the façade's plane. Four Ground Control Points (GCPs) were measured per façade and their coordinates were used for the sensor orientation. The latter gave the exterior orientation parameters of the images which in combination with the acquired imagery and the image matching algorithm were used to generate the digital surface model (DSM). The DSM layer is a 2.5D which represents the elevated features of the façade and it is later assessed for its quality. After that, the orthorectification of the images is done for geometrical corrections such as uniform scale. Again the resulted product will be assessed for its quality directly after the generation. If the quality condition is acceptable then the two products will be used as input data in OBIA to segment and extract the damage feature of cracks and holes.

At this stage the information that VHR images could provide (DSM & orthorectified image) will be further used for the OBIA. A hybrid approach for the segmentation process will follow. That means that the information of both orthorectified image and DSM was combined for the segmentation stage. For the current thesis this hybrid approach is the stage where the additional information from the DSM is expected to give more reliable and accurate information. The latter enabled the use of the elevation and colour information to identify and extract the damage features based on the two products but at the same time for the segmentation, it was also combined with the information from the RGB orthorectified image. The result of the segmentation is analysed based on previous studies results in combination with the current results. This way the parameters of the segmentation algorithms were adjusted for each material and a final value for each was selected. Thus, if a comprehensive segmentation is produced then the aim of the classification process is to assign in the segmented objects a respective class based on the predefined set of properties. The classification result will demonstrate the façade as a unique homogenous object and the potential damage in the classes as cracks or holes which then are used for the accuracy assessment. The final quality assessment of the classification is done based on a number of statistical measurement factors.

In the end, the structural expert or civil engineer will derive a classification result on an interface showing the highlighted damage feature in accordance with its geometrical properties such as the maximum width, length and area but also its location. Based on this information, the specialist will be able to add an essential quantitative characterization analysis tool for the SDA procedure. In addition, the time to generate SDA after the event will be decreased substantial and the danger of in situ inspections will be eliminated.

An alternative approach of OBIA is tested in parallel. A previous research done by Galarreta, (2014) on damage building assessment has been explored and the developed rulesets for damage detection and classification were implemented solely on the produced orthophotos of the damage samples of concrete and brick in order to test the transferability of previous rulesets on the current damage samples.

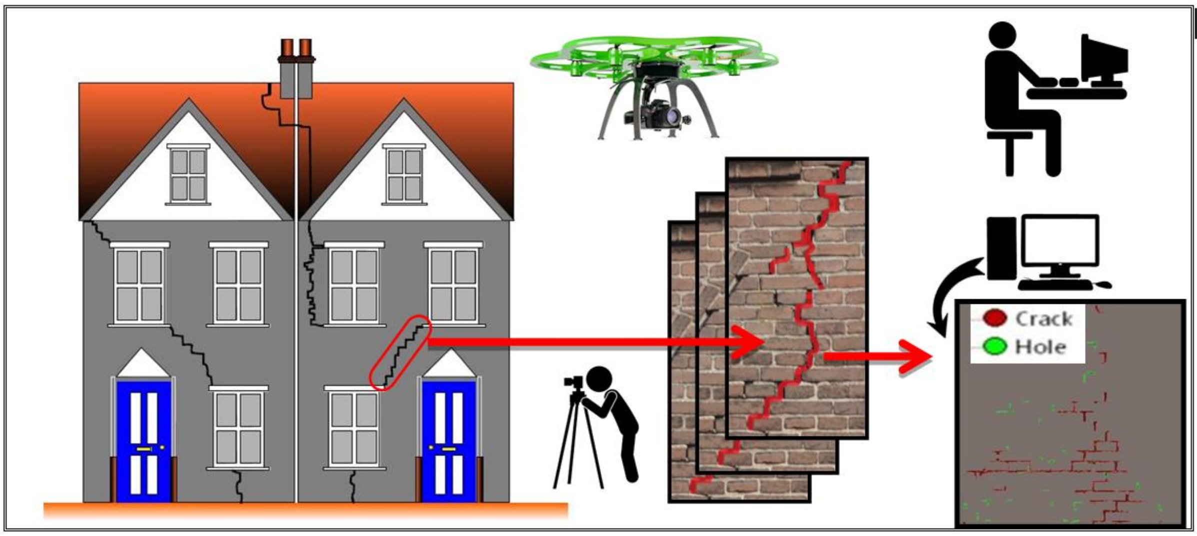

Figure 8. Conceptual model of image-based crack detection and characterization

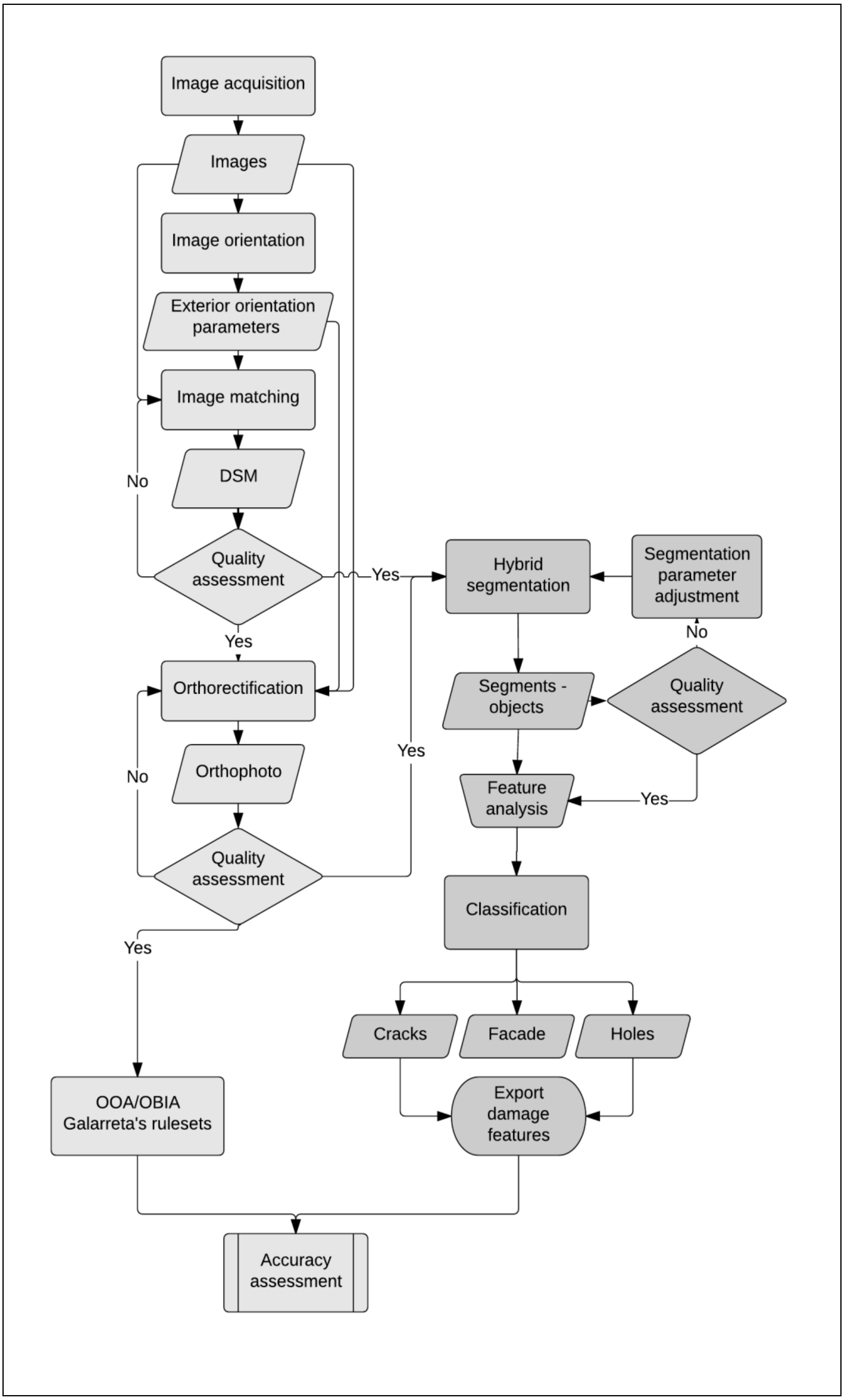

Figure 9. Flowchart of the research

3.1. Image acquisition

The process of data collection for surface damage features such as the cracks and the holes on buildings was implemented in three distinct stages, during daytime. Each stage represents a different damaged location for data acquisition. At the beginning of the experiment the following decisions for the following had to be taken:

- Site selection
- Platform
- Sensor.

For the site selection as it has already been mentioned already damaged buildings were selected in order to stimulate the after the disaster geometries. To find such building in the Netherlands were difficult as most of the times the restoration of the damage takes place immediately after that. The construction materials of the places where the images captured are a) brick, b) concrete and c) insulating material. This is because; the first two cases constitute the mostly used in building constructions and such were considered as the most representative. Concrete is defined as a mixture of cement, aggregate and water (American Concrete Institute, 2011). Brick is a traditional structural building material that is used extensively in the building construction in the north part of Europe for individual residential accommodation. Its ingredients are usually fine clay, brick and cement. (National Authority on Clay Brick Construction, 2014). The case of the insulating material was selected as it could give further possibilities at the quality assessment stage because of the TLS data that were additionally acquired.

The criteria for the platform were a) the availability, b) the cost and c) the accessibility possibilities that were provided. At the beginning the aim was to use a UAV that could easily and safely reach a disastrous site for VHR image acquisition. However, time and platform availability did not allow that. Instead, a terrestrial platform with a VHR sensor mounted on it was used. The sensor should be capable to acquire images of very high spatial resolution, at the level of few mm. This requirement derives from the geometrical characteristics of the object that is under the focus of the current study. Consequently, the sensor that was used is the digital camera NIKON D3200 DSLR with AF-S DX NIKKOR 18-105mm lens (Table 3).

All the experiments conducted with the same terrestrial platform and the same sensor which will be named in the thesis as digital camera C. For the image acquisition two different illumination conditions were tested. The photos were captured once with flash and then the same scene was capture without flash. This is because at the analysis stage the different result of the two cases should be examined in order to assess if the "with flash" images can provide more detailed information. The experimental settings are presented in Table 2 Specifically, for each sample areas (e.g. Brick I) 2 distinct datasets (M1a-M1b) are available after the image acquisition step, a) photos with the use of a flash light and b) photos under the ambient lightning solely.

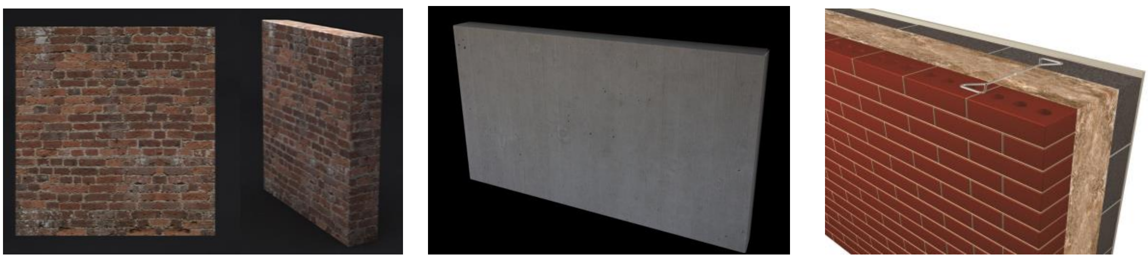

a b c

Figure 10. Materials: Brick (3dmodeling4business.com) -a, Concrete (tf3dm.com) – b, insulation - c

	Light / Material	Active Source	No additional illumination
Terrestrial platform	Brick I Brick II	Camera C Building material M_{1a}, M_{1b} Flash	Camera C Building material M_{1a}, M_{1b} No Flash
	Concrete I Concrete II	Camera C Building material M_{2a}, M_{2b} Flash	Camera C Building material M_{2a}, M_{2b} No Flash
	Insulating material	Camera C Building material M_3 Flash	Camera C Building material M_3 No Flash

Table 2 Experimental settings

The first dataset was captured in Enschede, Roombeek area (Figure 11). The study area suffered from a catastrophic fireworks explosion with many fatalities and heavy damage in 2000. The wall on which the crack was detected is part of the ruins of a damaged brick façade. After the image acquisition the crack was renovated in short time by the municipality of Enschede. The second area is a demolition site of an old factory in the city of Gronau, Germany with brick and concrete facades. The images of the third dataset were captured during an indoor experiment that took place under controlled indoor conditions in the faculty of ITC on a damaged material that is used for insulating purposes. Two facades made by brick and two made by concrete were captured in outdoor conditions. In Table 3 the material "Brick I" is illustrated from the area of Roombeek and the rest of the sample areas were found and captured in Gronau (Brick II, Concrete I and Concrete II) and indoors of the ITC faculty building (insulating material).

Figure 11. a) Study area in Gronau b) Study area in Roombeek, Enschede

3.1.1. Sensor

The sensor used for the image acquisition stage was a very high-resolution digital camera NIKON D3200 DSLR with AF-S DX NIKKOR 18-105mm lens (Table 3). For the analysis that will later be done in OBIA step, it was decided to capture two different sets of images per case. The first one would be without additional illumination while for the second one the flash light would be used. This is to test if further information can be extracted when the radiometry of the image is enhanced. For example, the additional illumination could solve the problem that shadows may cause within the crack but not the geometrical problems because of the occlusions. Moreover, the largest image format (6,016 x 4,000) among three different, of the camera was used to capture as many details as possible. In order to set constant parameters for the images and have similar errors (e.g. lens distortion), a constant value was defined for the aperture, shutter speed and focal length during the acquisition. For instance, a wide angle of 35mm was considered as constant focal length during the experiments.

Effective Pixels	24.2 million
Sensor Size	23.2 mm x 15.4 mm
Image Sensor Format	DX
Image Area (pixels)	**(L) 6,016 x 4,000 (3.8μm)** (M) 4,512 x 3,000 (5.1 μm) (S) 3,008 x 2,000 (7.7 μm)
LENS INFORMATION	AF-S DX NIKKOR 18-105mm f/3.5-5.6G ED VR
Focal Length Range	18-105mm
Maximum Aperture	f/3.5
Flash properties	Shutter speed (max): 1/200sec
VR (Vibration Reduction) Image Stabilization	

Table 3. Sensor characteristics

3.1.2. Experimental setup

The data acquisition was a crucial part in the current research (Figure 12). At first, an extensive work at the office was carried out to identify damaged areas that could be investigated to collect the damage information. The aim was to find facades that will constitute the base data of the study of the representative materials. When the damaged facades were selected the image acquisition was conducted. Artificial targets were created and printed in advance. These targets were attached on the façades to be used as GCPs for the sensor orientation. These points could not have been randomly placed on the façade but should shape an orthogonal as they were also used for the definition of the local coordinate reference system. The targets were removed after the image acquisition. Due to inaccessibility in some areas the image acquisition met some limitations such as difficulties to establish the GCPs on the building.

In the following step, multiple images were captured with an approximate baseline of 10-20cm to generate the 3D products that are going to be used in the image processing step. As a result, the image overlap exceeded the 80% which is sufficient for this case. If the disaster site is inaccessible from human experts for instance after a disaster in a nuclear plant then an airborne platform will take the place of the specialists. The use of a UAV platform to perform a predefined flight path to capture damage features on high elevated infrastructure such as power plants tubes or installations will be time and cost efficient plus it does not put in danger the experts.

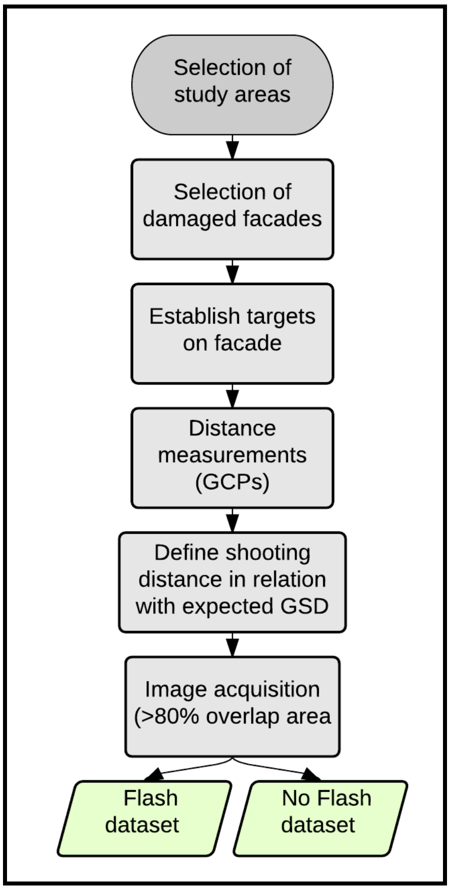

Figure 12. Image acquisition setup

Multiple shooting distances were explored during the image acquisition (Table 5) to lead to better results in the process of image matching. In some cases, such as "Concrete II" the shooting distance was in particular 3m due to the site difficulty of establishing more suitable positions. Also, for the last damage sample, the "Insulating material" the shooting distance was approximately 2.30m due to predefined constant height of the material in the tested area.

Furthermore, in order to have reference ground truth data of the studied cracks, manual point measurements were carried out during the field visit to explore the maximum width and maximum depth of the objects of interest. (Table 4)

ID	Max width	Max depth
Brick I	1.2cm	2.3cm
Brick II	2.5cm	6cm
Concrete I	3.5cm	3cm
Concrete II	2.5cm	2.5cm
Insulating material	4.1cm	2.5cm

Table 4. Manual measurements of cracks

Image	ID	Location	Illumination	Nr. of images	Weather conditions	Shooting distance	Focal Length (mm)	GSD (mm)
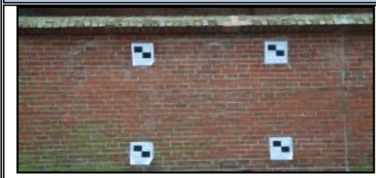	Brick I	Roombeek	Flash	29	Cloudy	5m, 6m	35	0.5
			No Flash	85				
	Brick II	Gronau	Flash	63	Cloudy	4m, 5m, 6m	35	0.5
			No Flash	71				
	Concrete I	Gronau	Flash	38	Sunny-Partial Cloudy	5m, 6m	35	0.6
			No Flash	45				
	Concrete II	Gronau	Flash	28	Sunny-Partial Cloudy	3m	35	0.3
			No Flash	23				
	Insulating material	ITC	Flash	13	Indoor	2.30m	35	0.3
			No Flash	13				

Table 5. Inventory of terrestrial image acquisition stage

3.2. Image post-processing

After the image acquisition stage the post-processing procedure of the selected imagery is done. For this study Pix4D was the software that was used for the photogrammetric part of the thesis but in real case scenario any other photogrammetric software could support this part. After the photogrammetric a series of data inspection mostly for quality assessment, completeness and correctness was done. At the end the photogrammetric data were the input for the OBIA task.

3.2.1. Photogrammetric procedure

Pix4D that constitutes a semi-automated image processing software specialized on UAV datasets for mapping and modelling purposes was used for this case. The input data were the different sets of the acquired imagery, the interior orientation parameters of the sensor and the coordinates of the GCPs at the arbitrary local coordinate reference system. One of its greatest advantages is that it can produce automatically the orthorectified image and the DSM of remarkable high quality based on the dense image matching technology (Pix4D, 2014).

In general, the data processing in Pix4D is conducted in 3 steps. At first the project set up with all the relevant parameters (e.g. interior orientation) is done, then the GCPs measurements on the images and at the end the bundle adjustment for computing the exterior orientation parameters. During the last step the extraction and matching of the feature keypoints among the images is processed. The current step is critical in terms of the accuracy (completeness and correctness) of the output. If the overlap of the imagery is less than 60% the matched points among the images will not be enough for a high accuracy result. In the current experiment the area overlap exceeded 80%. After the procedure of the point densification and filtering the image based point cloud of the area is produced. This DSM is later used for the orthorectification of the images. At the end of this step the input for the OBIA data are available.

The current software has been used to produce accurate orthophotos and Digital Surface Model (DSM) of the overlapping images that acquired. For each material that was tested, two orthophotos and two DSMs were created. Each pair of images per material represents the image acquisition step under the ambient illumination solely and the other represents the same area but with the enhanced illumination from the camera's built-in flash.

Figure 13. Pix4D concept (Pix4D, 2014)

3.2.1.1. Digital Surface model (DSM)

DSM is the digital elevation model that represents the height of the objects that lay on the earth's surface. More specifically, it comprises the elevation of all natural and man-made objects such as buildings, vegetation, roads etc. For the current case the objects are not on the earth but on or close to the facades plane.

The purpose of DSM generation is to derive a complete 2.5D model of the building's surface (façade) including also discontinuities such as potential damage features that are represented as less elevated regions in the surface model compared with the background (façade). However, due to that automatic image matching algorithms it is not able to differentiate between artificial and natural objects the outcome is a 2.5D DSM of the façade. The latter will be the input data to generate the orthoimage of the surface. In Figure 15 the DSM of the sample area "brick II' no flash.

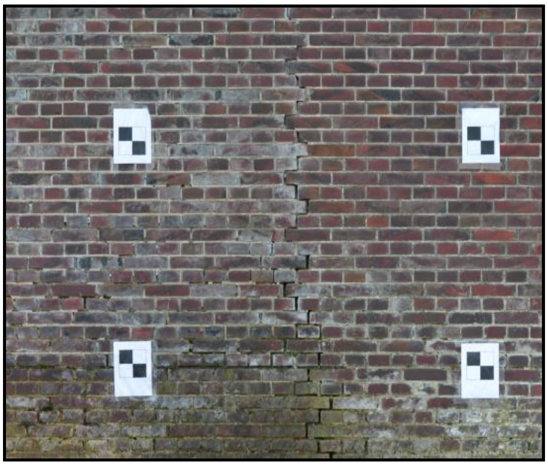

Figure 14. Orthorectified image of sample "brick II" no flash

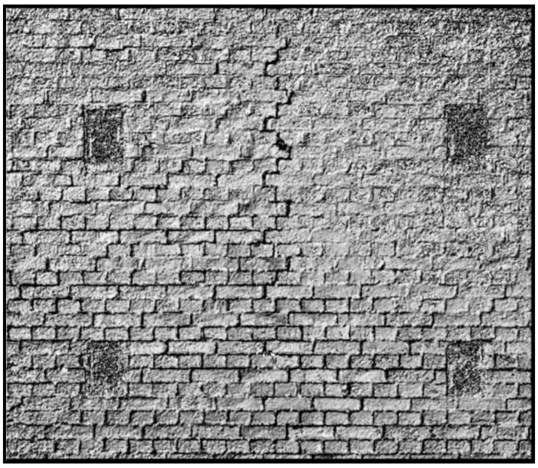

Figure 15. DSM of sample "brick II" no flash

3.2.1.2. Orthophoto

Orthophoto or orthoimage constitutes an image which has been geometrically corrected (orthorectified) in order to obtain a uniform scale and eliminate relief displacements affects and distortions that can be caused for example from the lens. This product can be used for accurate geometrical measurements (e.g. distance) that will contribute to the analysis in OBIA. In the current research, orthophotos refer to georeferenced output products from VHR overlapping imagery. The orthophoto in the current research will be used as input data in the OBIA stage to proceed with the hybrid segmentation process. At the step of the hybrid segmentation the three layers (bands) will be given separately and the spectral resolution of each layer will contribute to the segmentation. In Figure 14 the orthorectified image of the sample "brick II" no flash is illustrated.

3.2.2. Data inspection and analysis

The data used for this study but also the data produced during the study were inspected and occasionally analysed in several softwares. In order to visualize and assess the quality of the output two software tools have been used, Cloud Compare and Global Mapper. Cloud Compare (CC) is an open source 3D point cloud processing software. Its main purpose is to detect changes in 3D high density point clouds acquired with laser scanners. (Danielgm, 2014). Global Mapper is an easy-to-use GIS software that offers access to an unparalleled variety of spatial datasets and provides right level functionality for all the potential users. It is a strong spatial data management tool which the only disadvantage that is commercial application. (Geographics, 2014) For the purposes of the current study a student trial licence was employed for 60 days.

For example one of the tasks conducted via this software, in order to eliminate and exclude parts on the two products that are not needed in the current research such as surrounding ground or tree branches, was the cropping of the DSM and the orthorectified image. The current procedure could have been avoided with the development of an extra ruleset to eliminate those points in the imagery but it terms of time it was not efficient.

3.2.3. Object-Based Image Analysis (OBIA)

As it is mentioned in chapter 2, OBIA includes two major steps, the segmentation and the classification process. The tool that was carried out the image analysis step is eCognition Developer 9.0 software package developed by Trimble (2014). The latter is the most used software package for OBIA techniques as more than half of the published papers in the domain of OBIA are making use of this software (Blaschke, 2010). Moreover, it offers a wide variety of segmentation algorithms from knowledge driven methods (top-down) to data driven methods (bottom up). In our experiments the multiresolution segmentation (MLS) was applied which is a bottom-up, region merging technique based on homogeneity criteria between adjacent pixels.

In addition, in our case the objects of interest are appearing in different scales in the imagery. As a result, MLS is capable of taking into account its variety and adapt the scale to fit the scale of the given task. Thus, it produces large homogenous segments in an arbitrary resolution in different type of datasets. In MLS, three factors have to be determined the scale, the colour and the shape. The colour can be weighted between 0-1 and the shape factor follows the same weight range between smoothness and compactness. Also a weight assignment between the used spectral bands or layers of the imagery is possible. The scale defines the maximum size of the object as a result, the process ends when the scale factor exceeds this value. The segmentation process was followed by a spectral difference segmentation to merge neighbouring objects based on their mean layer intensity values (Trimble, 2014a).

The current chapter is divided in two steps. In the first step an extended analysis is performed of a previous related research (Galarreta, 2014) in ITC faculty on building damage assessment. In the mentioned research of Jorge Fernandez Galarreta the developed rulesets on OBIA for damage detection were adopted to test them on the acquired images of the current research.

In the second step an independent series of rulesets were designed in the context of the current research to identify and classify the damage features as cracks or holes. Different rulesets were created for each of the materials that were under investigation.

3.2.3.1. Implementation of Galarreta's rulesets

In order to test the applicability of OBIA rulesets of Galarreta's research, the rulesets for damage detection and classification were implemented on the damaged façade samples that were acquired during the field visits in Enschede and Gronau. Due to the fact that the mentioned rulesets were designed for single imagery, we used solely the produced orthophotos of the damaged facades. The implementation was done in steps in order to demonstrate the applicability of each step in the ruleset. The main difference of Galarreta's research is that the designed set of rules is based on single RGB imagery when the current research is using as input a 2.5D DSM and the orthorectified image.

In Galarreta the OBIA stage was divided in 4 distinct stages according to the researcher:

a) Segmentation process: The followed approach was including a sequence of two segmentation algorithms, the multiresolution segmentation followed by the spectral difference segmentation step. The selection of the parameters' value was done by a number of trial and error experiments.

b) Feature analysis: An exploitation of the objects' characteristics was followed in order to find out the appropriate spectral, spatial and contextual information that the classification can be based on for the next step. The selected damage classes were holes, cracks and interaction of cracks with structural elements.

c) Classification process: The aim of the current step was to assign a meaningful class to the segmented objects that resulted from the previous process. A set of rules were designed based on a number of object's characteristics after the feature analysis step to fulfil the aim of the classification. Some of the selected objects' characteristics are; area, asymmetry, rectangular fit and compactness

d) Export: In the last step, the classified objects were exported in a vector format in order to proceed with the quality assessment of the classification.

The aim of the current test was to check if the current research could be based on what previously was done and continue the development from that stage on. Unlikely, the results were not successful and this is why another approach should be adapted.

3.2.3.2. Object-based Image analysis of damage features

In the current step a set of rulesets were designed to capture the damage features of interest on a façade level and classify them accordingly. For the purpose of damage classification two damage classes were created after careful consideration based on literature and extensive discussions with the experts, a) holes and b) cracks. The aim of this step was to develop a set of rulesets capable to capture the location of damage features, classify the segmented objects in the predefined damage classes and extract the damage information. The developed ruleset had to be able to be transferred and applicable for different damage scenarios.

We follow a hybrid approach to segment the imagery by using the 2.5D DSM and the orthophoto of the damaged facades. First, the image-based DSM was the first input and it includes all the damaged artefacts of the façade which are visible as degraded cavities. The orthorectified image was the second input of the hybrid approach where the damaged features are visible and appear with low brightness value. This is because there are shadows in the damaged area. Based on this assumption for the damage features the rulesets were designed to fulfil the segmentation process in order to highlight the cracks and holes and keep as a homogeneous intact object the "healthy" façade.

The classification process which followed after the segmentation has the aim of assigning the objects in meaningful damage classes. A set of rules were designed to fulfil the classification requirement based on careful selection of the object's characteristics like the ratio length to width, the rectangular fit and the area. The approach of parameter selection was motivated from previous works on building damage assessment in OBIA such as from Galarreta, (2014), Blaschke, Lang & Hay, (2008) and Mavrantza & Argialas, (2008). However, the major difference between the current approach and the previous study that was done in ITC by Galarreta is that the hybrid approach that was adapted takes advantage of the 2.5D information that the DSM provides. Specifically, for this study three different rulesets were designed in order to cope with the three different constructing materials (Appendix 7.4.2).

3.3. Accuracy assessment

The accuracy assessment is a procedure for quantifying the quality of the extracted damage features in terms of completeness and correctness and it constitutes a critical part of the post-classification stage. It is usually done by comparing the classification result with reference data that is considered as the most accurate. Sources of reference data can for example be ground truth measurements, images of higher resolution, maps or laser scanning data. For the current case the orthorectified images and the point cloud data from a laser scan were used as reference data.

3.3.1. Area based approach

The first accuracy assessment approach was area-based (Joshi, 2010).. Every image was examined in order to check the quality of the identification and classification of damage features. Statistical measurements took place between the extracted area from OBIA and a reference data that was previously created by manual digitization of the selected damage features on the orthophotos in ArcGIS (ESRI, 2014) after their generation.

In Figure 16, an assumption is made; the rectangular ABCD is the reference data and the rectangular SROP is the extracted damage features area from the OBIA methods. Then three types of measurement factors could be defined. The green area or True Positives (TP) is the area which is present in the reference data but also in the extracted one from OBIA. Next, the blue area or False Positives (FP) is the area that is present in the reference dataset but not in the OBIA result. For instance, cracks that were identified as cracks in the manual digitization is not present in the post-classification stage. The red area or False Negatives (FN) is the area that was extracted as damage feature from the classification step but it was not present in the reference.

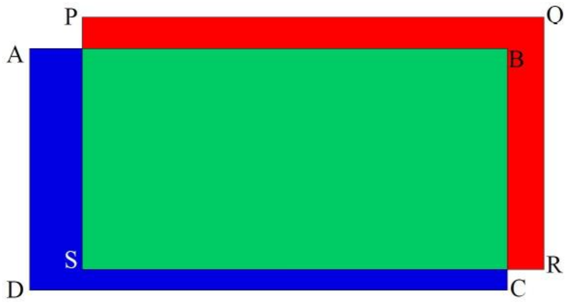

Figure 16. Illustration of the accuracy assessment (Joshi, 2010) Green: TP, Red: FN and Blue: FP

Split factor = TP / FP

Missing factor = FN / TP

Correctness = TP / (TP + FP)

Completeness = TP / (TP + FN)

Figure 17. Factors for performing the accuracy assessment (Joshi, 2010)

Based on the previous three factors, four quality measurements could be obtained (Figure 17) to represent the quantitative quality analysis of the classification.

First, the split factor represents the amount of true positives compared with the amount of false positives. Second, the missing factor represents the amount of false negatives compared with the amount of true positives. The latter is a measurement factor to indicate the amount of missing information after the classification. Third, the correctness is a measure factor which represents the correct detection rate against the reference damage features. It ranges from 0-1 and it is represented in percentage (%). It is a factor which indicates if the reference damage information was correlated accurate with the classified damage features. Completeness is a factor which indicates how complete the extracted damage features are and it ranges from 0-1 like correctness factor.

As it was time consuming to run the spatial queries in ArcGIS every time for each set of data, a script was developed in R-project to automate the procedure of accuracy assessment. As an alternative accuracy assessment method and in order to automate the procedure, a script was designed in R environment (Bell Laboratories, 2014). R-project is a programming language based on a variety of scripts and environment for statistical computing and graphics (R Core Team, 2014). The developed script is given in appendix 7.3.

The developed script in R first calculates the area of the reference data and the difference between this and the ArcGIS approach is the generation of a buffer zone of 0.05cm around the objects. The buffer zone is created to eliminate errors because of small areas near the feature's boundaries that had to be included as damage feature areas during the manual digitization. The digitizing process was done in order to define the truth crack on the orthophoto (reference data). The reference area with the buffer is calculated and the intersection with the area of the objects resulted from OBIA is computed. Following this approach the accuracy assessment of the classification could be done in a more automated way that allows more tests for the quality assessment. This script used to assess the accuracy for the damaged cases in insulating material and brick. The main reason of the current script development was that the latter is less time consuming to implement the accuracy assessment.

3.3.2. Point based approach /Laser scanning – LiDAR:

LiDAR or Light Detection and Ranging is a remote sensing technology that enables the user to produce accurate three dimensional point clouds of a surface without direct contact (Minehane, Donovan, Ruane, & Keeffe, 2013). The acquisition can be performed from a terrestrial and/or an airborne platform. The latter is a lightweight survey instrument which produces fully linear unidirectional and parallel scan lines even under limited space conditions as the one that were in the current experiment (Riegl, 2014). The acquired point cloud was processed in a software tool called RISCAN PRO designed particularly for the RIEGL laser scanners.

In the current thesis, the laser scanner was performed for the indoor case in order to produce a validation dataset for point based accuracy assessment. A 3D terrestrial laser scan of the structure was carried out in December 2014 on the insulating sample using a RIEGL VZ-400 (Figure 18) laser sensor and produced a dataset with a point density of 25 points/cm^2. The current laser sensor is able to measure the geometrical properties of the crack with high positional accuracy.

This dataset was used as reference for this point based approach. First, it was co-registered with the image-based DSM and for this registration common points were used as GCPs. Then in Cloud Compare software the two co-registered point clouds were analyzed and the results of the comparison showed no substantial differences between them. That validates the high accuracy of the image-based DSM that was used for the OBIA. After, the result of the comparison it was decided that only the image-based DSM will be used for the OBIA, as the point cloud from the TLS did not provide additional information, at least for the insulating material.

Next, the point cloud was used to assess the geometric accuracy of crack's length. On the TLS point cloud 10 different users were asked to point out the end points of the crack based on the assumption that the length is the distance between the two end points of the visible crack region. A reliable dataset was then available to calculate the reference length of the crack. The latter was compared with the one resulted from OBIA. Due to time limitations there was not the possibility to collect validation datasets for the rest of the damaged samples.

Figure 18. Laser scanner RIEGL VZ-400

4. RESULTS

In the current chapter the results of the proposed methodology are presented. This chapter is structured the same way like the methodology chapter in order to link each procedure with the results the derived results and their quality. First, image acquisition is explained followed by the generation of the DSM and orthophoto and then, OBIA process is presented with the extracted damage features that were assessed for their quality.

4.1. Image acquisition

The image acquisition process was implemented in multiple steps in order to collect the appropriate datasets from damaged facades. The current step produced a large number of photos, different for each sample area. After careful consideration, some of the collected images were neglected due to blurriness and a number of approximately 25 images have been chosen to be used as input for the photogrammetric procedure. The DSM and orthophoto were generated based on these selected images. After, the collection of the imagery, an inventory was created (Table 5) in order to have a holistic perception of the obtained datasets. The designed data acquisition framework was one of the objectives in this research in order to develop a reliable concept to collect appropriate data for further damage identification.

4.2. Photogrammetric data

After the image acquisition, the photogrammetric procedure was completed. The results of this step were a) the image-based DSM and b) the orthorectified image of each sample area. From the inventory created after image acquisition, 10 datasets were available for further analysis (Table 6). In particular, as mentioned earlier, for each selected damage site (e.g. Brick I), two sub datasets were produced one with the flash light and one under the ambient illumination during the day of acquisition. In Table 6, all the generated datasets from the photogrammetric procedure are presented with the spatial resolution respectively. In appendix 7.1 & 7.2 the produced orthophotos and the DSMs can be found for each damage sample.

ID	Output	Details
Brick I	DSM	Grid size: 0.5 mm
	Orthophoto	GSD: 0.5 mm
Brick II	DSM	Grid size: 0.5 mm
	Orthophoto	GSD: 0.5 mm
Concrete I	DSM	Grid size: 0.5 mm
	Orthophoto	GSD: 0.5 mm
Concrete II	DSM	Grid size: 0.4 mm
	Orthophoto	GSD: 0.4 mm
Insulating material	DSM	Grid size: 0.3 mm
	Orthophoto	GSD: 0.3 mm

Table 6. Photogrammetric data

4.3. OBIA

The current chapter of OBIA was divided in two sub-sections. First the implementation of OBIA rulesets of a previous research on structural damage assessment on the damaged samples of the current research is illustrated and explained in details for two different scenarios (concrete facades and brick facades). As it has been mentioned that was done in order to assess the possibility to adapt the previous OBIA rulesets for the hybrid approach. At the beginning this ruleset was not edited in order to assess the result from the current dataset. If this result would be successful then the ruleset could have been adapted in order to use the DSM, as well. However, the result was not the expected and in the second part, the description of the developed OBIA rulesets for three different scenarios (concrete facades, brick facades and ITC insulating material) under the current research are demonstrated and explained.

4.3.1. Galarreta OBIA rulesets

In Galarreta's thesis, three different rulesets for individual materials (concrete and brick facades and roofs) for feature damage extraction have been developed. Due to the fact that this approach was designed on building level, in the current research there was not presence of roof samples and thus the ruleset designed for damage extraction on roofs was neglected. The rulesets were designed to fulfil the requirement of highlighting objects that did not fit with their regular environment and illustrate potential damage elements on the three mentioned materials. In order to test the applicability and stability of the developed rulesets they have been applied step by step on the orthophoto products of the current research.

The results showed that the current test was not successful as the designed rulesets were developed in order to generate information based only on the orthorectified image. That means that other parameters were considered in order to conclude if an object was damage feature or not. Also, the ruleset was mostly based on geometrical properties of the damage feature in combination with semantics for the windows and pillars that don't exist in the new images. Also, parameters like brightness of the object were not included in this ruleset. Moreover, the height information of the façade plane was not available in the OBIA process. The results of this test indicated that a new set of rules should be designed.

4.3.1.1. Reinforced concrete samples

In the current section the already designed rulesets of previous research were tested on the new dataset.

Segmentation process: The segmentation process was divided in two sub stages. First a multiresolution segmentation (MLS) algorithm was applied followed by a spectral difference segmentation algorithm in order to merge the neighbouring segments based on their mean layer intensity values (Table 7). The selection of high values for the shape and compactness parameters is based on the researcher's assumption that the segmentation process will capture the big homogenous parts of the façade but at the same time the small holes and cracking features will be identified. The choice of value 20 in the spectral difference segmentation allowed similar segmented objects to be merged and keep intact the ones that are contrasted with the background.

Algorithm	Parameter	Value
Multiresolution segmentation	Scale	100
	Shape	0.8
	Compactness	0.5
Spectral difference segmentation	Spectral difference	20

Table 7. Segmentation parameters for concrete facade (adapted by (Galarreta, 2014))

In Figure 19(left image), the result of the multiresolution segmentation algorithm is illustrated followed by the spectral difference segmentation result. There, the concrete façade was over segmented on the MLS step but with the spectral difference algorithm (Figure 19 right image) similar objects were merged and the essence of the damage was captured except from a continuous object in the down part of the image which was segmented wrongly as individual object. Due to high complexity of the concrete facade many artificial objects were captured as individual damaged segments.

Figure 19. MLS result (left) on the sample "concrete I" spectral difference segmentation result on the sample "concrete I" (right)

Classification process: The following step was to classify the segmented features based on their parameters. These parameters are; the ratio width to length, the compactness, the relative border and the area. The aim of the classification process was to assign the objects in one of following classes; windows, structural elements, façade and cracks. In the new samples the structural elements such as building columns and windows were neglected due to their absence on the imagery. The final result of the sample area "concrete I" is illustrated in Figure 20. The elements that were characterized as cracking features are highlighted with red colour.

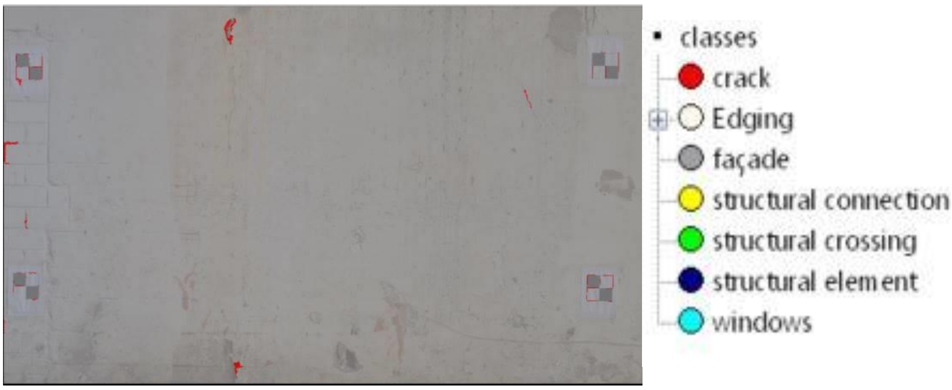

Figure 20. Final result of the classification in the image “concrete I”

The features that were identified on the concrete sample were only small parts of the existed cracks. Also there were some misclassified objects as cracks where in reality they were the GCPs that were attached on the façade. From the current result it is concluded that the rulesets developed for concrete facades by Galarreta are not completely transferable in the current damage samples.

4.3.1.2. Brick samples

Segmentation process: The same strategy as in the concrete was followed in the brick samples. In the first step, a multiresolution segmentation (MLS) algorithm was applied followed by a spectral difference segmentation algorithm but with lower values for the parameters of scale, shape and compactness. This was done in order to capture the essence of damage more precise on the individual bricks. According to the researcher, the ruleset in the brick samples was made to identify features such as holes, cracks and interactions of cracks with structural elements (Table 8). The aim was to capture the individual intact bricks but at the same time to highlight the essence of damage like holes and cracks among them. On contrary with the concrete material the value for the spectral difference algorithm was higher due to the high heterogeneity among the bricks.

Algorithm	Parameter	Value
Multiresolution segmentation	Scale	25
	Shape	0.2
	Compactness	0.2
Spectral difference segmentation	Spectral difference	35

Table 8. Segmentation parameters for brick façade (adapted by (Galarreta, 2014)

In Figure 21, in the left image can be seen that the "brick II" sample was over segmented after the MLS step. In the right image the resulted segmentation is illustrated after the implementation of the spectral difference segmentation algorithm. On the latter, can been seen that bricks were identified as individual objects and areas that were representing with grey colour are the background of the façade.

The current procedure enables the user not to miss any detail that could be proven as damage indicator but on the other side the high heterogeneity between the individual bricks produced a messy segmentation result. In addition, the current crack on the brick material can be considered as complex case due to the fact that the mortar joints among the bricks could be confused as crack regions in the detection of the damage. This is a problem that could be possibly be solved with the use of the height information.

Figure 21. MLS segmentation on the sample "brick II" (left) and spectral difference segmentation result on the sample "brick II" (right).

Classification process: The first step prior to any further classification was to create a binary classification step between the potential damage features and the façade (Figure 22). By using solely the object's attribute of area of the objects the mentioned classification step distinguished the areas of interest in potential damage (red colour) and façade (grey colour) in figure below. Furthermore, the binarization was implemented to neglect bricks that were classified as damage due to their size.

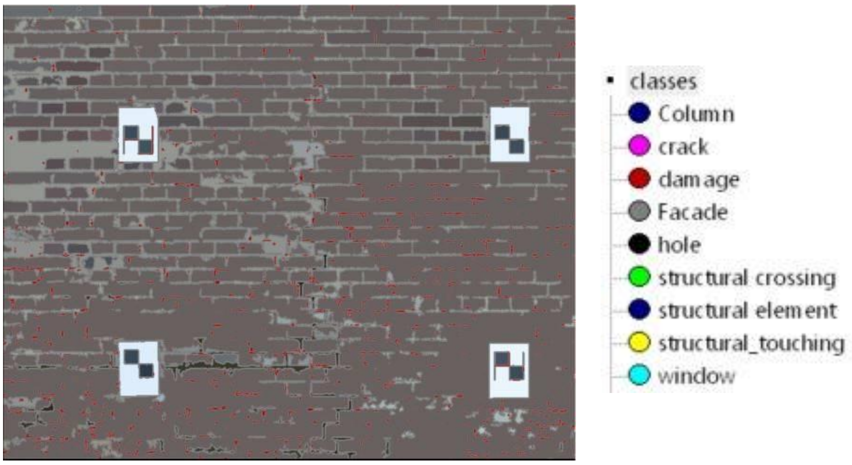

Figure 22. Result of the binary classification in the image “Brick II” no flash

In Figure 23, the result of the final classification in four different classes can be found. First, the cracking features are illustrated in pink colours and the façade is represented in grey colour as background. Holes are represented by black colour and there are some cyan objects that are misclassified as window objects. The current ruleset includes a small refinement process in order to get rid of the mortar (concrete lines) between the bricks. In order to fulfil the previous assumption a threshold of 5.6 in the ration length/width was used. Due to the high complexity of the brick facades the resulted classification is messy and the applied rulesets were inappropriate to highlight the cracking features on this type of material.

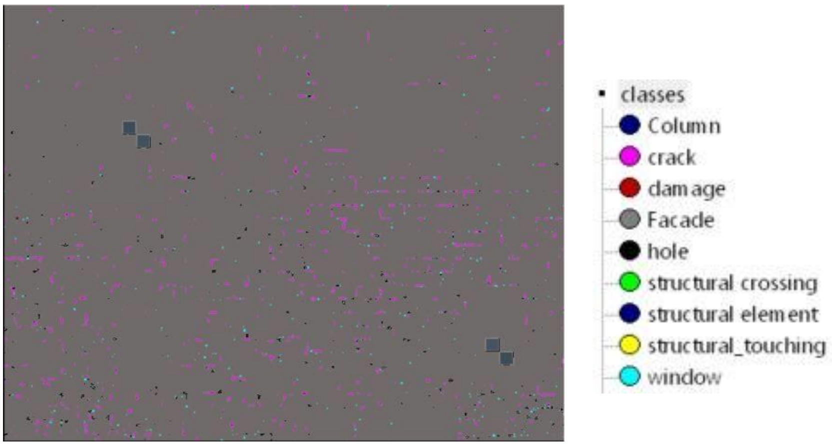

Figure 23. Final result of the classification in the image “Brick II” no flash

4.3.2. OBIA rulesets

In the current subsections, a detailed analysis is provided of the selected damage features and an explanation of the developed rulesets for each material (concrete, brick and insulating material) is provided. As explained in the chapter 3, an extended literature review on damage features and several discussions with experts on the field of building damage assessment the damage features that were selected to sort the damage classes based on the imagery were; (Figure 24):

- **Cracks**
- **Holes**

These features could be found in all the damage samples that were investigated in the current research. Since the aim of the current step is to extract the damage features, after visual interpretation of the scene and feature properties analysis, a series of rulesets were designed in order to capture the essence of damage. Cracks are defined as elongated damaged features that are less elevated from the rest of the background (façade) due to the deterioration process and they appear darker because of the shadows within the damaged area. All the developed rulesets for damage extraction were based on the same concept. The damage elements were objects that did not fit with the rest of the background based on a variety of properties such as the elevation of the objects and/or their brightness value.

Figure 24. Left image, an example of a crack feature. Right image, an example of a hole feature.

4.3.2.1. Reinforced concrete samples

All the concrete samples were attempted to be analysed with the same approach as a result the same ruleset was implemented in both "Concrete I" and "Concrete II" samples in order to identify elements that define potential damage such as holes and cracks. The designed ruleset is represented in details in the appendix (7.4.2).

1. **Segmentation (Concrete I)**

The segmentation process was done by combining two segmentation algorithms that are available in eCognition (Trimble, 2014a). The first is the MLS, a bottom up algorithm based on spectral and shape homogeneity criteria and the second is a spectral difference segmentation algorithm. The selected parameters for the two algorithms are presented in Table 9:

Algorithm	Parameter	Value
Multiresolution segmentation	Scale	90
	Shape	0.2
	Compactness	0.2
Spectral difference segmentation	Spectral difference	10

Table 9. Segmentation parameters for concrete material

The selected scale parameter on MLS for the concrete samples was high in order to deal with the high complexity between the sample areas but also to collect the essence of damage without missing any important information. The shape and compactness parameters were chosen to be low with a value of 0.2 in order to identify clearly the size variety of cracks and also small holes that could be the initial stage for crack propagation. The spectral difference algorithm was processed with a value of 10 in order to merge similar objects based on their mean layer intensity values but keep the ones that are contrasted with the rest of the background. In Figure 25, the result of the two segmentation steps is presented.

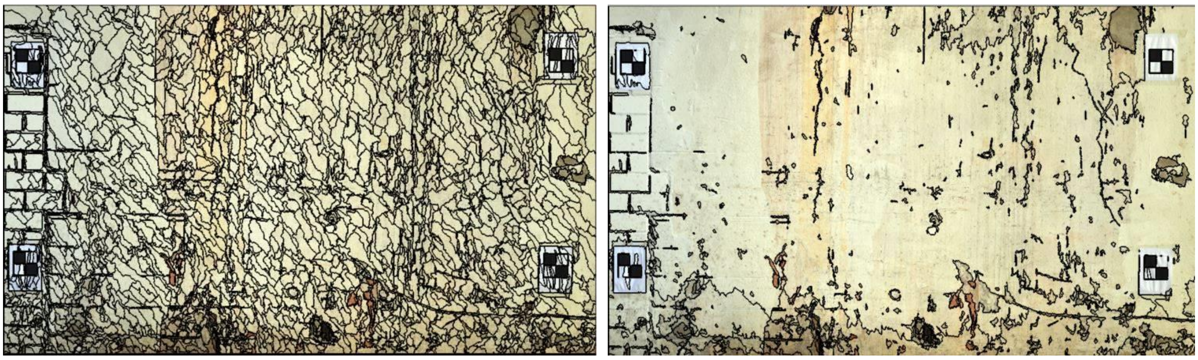

Figure 25. MLS result "Concrete I" sample (left). Spectral difference segmentation result (right)

From the above images it is clear that the result of the algorithm sequence is over-segmented and this needs to be treated later in the classification step.

2. **Classification**

After the segmentation process the aim of the following step was to assign to the objects one of the predefined classes. First, the images were divided in two classes (potential damage – façade) as a binary classification in order to eliminate artefacts that were classified as damage. The process was based on the use of the 2.5 DSM where the potential damage is represented as less elevated object and as a low brightness region in the orthophoto. As a result, objects that had less than 328 brightness value and a DSM value of less than 1000.4 were classified as potential damage and the unclassified as façade. The above thresholds were selected after feature analysis of the segmented objects and use of prior knowledge of the damage features. As shown in Figure 26 the holistic potential damage (holes and cracks) is illustrated with the blue colour and the rest of the background is merged and classified as façade.

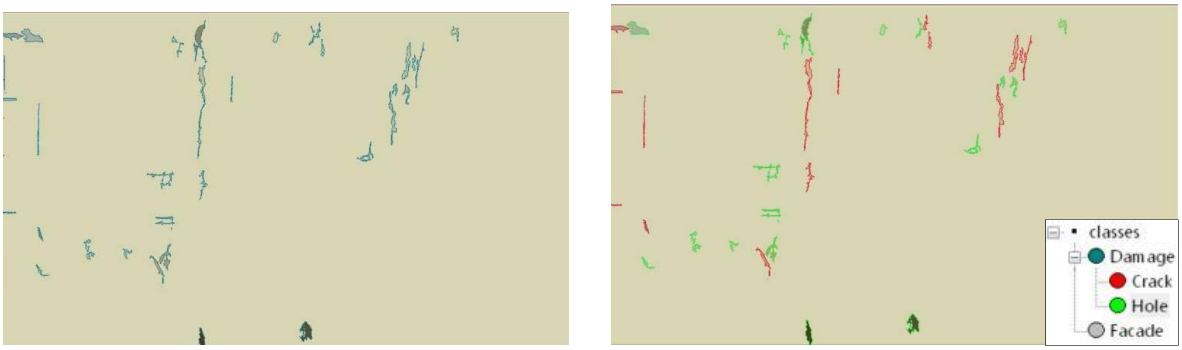

Figure 26. On the left an example of the binary result between "damage" and "façade" on "Concrete I" (no flash) sample. On the right, the resulted classification in cracks and holes.

The result of the binary classification showed that the developed approach to eliminate the artefacts was successful. Also, the contribution of the height related information was high and this can be proved from the comparison of the results of Galarreta segmentation (Figure 20) and the current. The last step of the classification process was to characterize the "Damage" objects further as holes or cracks. Based on the objects' characteristics such as the ratio length/width, rectangular fit and compactness the damage objects were divided in "crack" or "hole" features. More specific, a ratio value of more than 3 in combination with a rectangular fit value of less than 0.5 was used to characterize objects as cracks. The rest of the unclassified "damage" objects were assigned as holes. In Figure 26 right image, the resulted classification is illustrated with the respective damage classes, cracks and holes.

The same designed ruleset was implemented in the same sample area but in the dataset with the flash use. The result is illustrated in Figure 27 where it could be pointed out that a significant part of the cracking feature was identified in the upper middle part of the imagery with the use of the flash light. Moreover the use of the flash light identified less damage features compared with the no flash dataset. However, the target used as GCP was misclassified as "hole" and a hole feature that is present in the upper part did not being detected as it should.

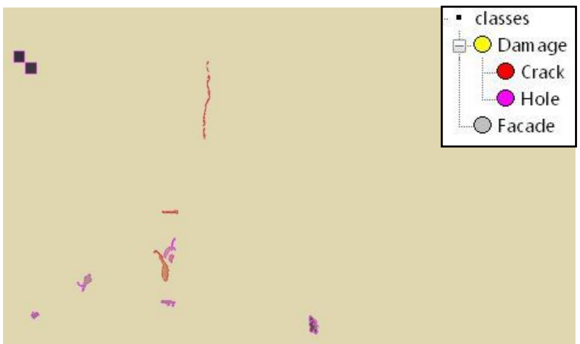

Figure 27. Result of the classification in "concrete I" with the flash light.

"Concrete II"

The second concrete damage sample was the "concrete II" where a visible crack was present on the upper part of the image. The parameters for the binary classification were modified as the facade level was different. Also the threshold for the brightness was estimated after feature analysis. Specifically the threshold values for the brightness was 291 and the mean facade height was 1000. In Figure 28, the resulted classification with the modified ruleset. The modified ruleset can be found in details in appendix 7.4.2.

Figure 28. Result of the classification in "concrete II" with the flash light (left) and with no use of flash (right).

4.3.2.2. Brick samples

All the brick samples were analysed following the same approach. The same ruleset was implemented for both Brick I and Brick II (flash – no flash) samples in order to identify elements such as hole and cracks on the bricks' surface or among their connections (mortar joints). The designed ruleset was divided in two main steps, the segmentation and classification process.

1. **Segmentation (Brick II)**

All the brick facades were attempted to be analysed with the same developed ruleset. The aim of the current ruleset it was to highlight signs of damage on the brick surface such as holes and cracks that are passing through the mortar joints or/and the individual bricks. It has to be mentioned here that designing specific rulesets for each of the "Brick" sample areas could lead to better and more accurate results due to high surface complexity of the sample areas and differences on the arbitrary coordinate system.

Algorithm	Parameter	Value
Multiresolution segmentation	Scale	25
	Shape	0.2
	Compactness	0.2
Spectral difference segmentation	Spectral difference	15

Table 10. Segmentation parameters for brick material

From Table 10, a value of 25 for the shape parameter was selected in order generates smaller objects than the ones in concrete due to the pattern of brick masonry. The shape and compactness parameters were selected with a low value of 0.2 in order to capture the individual intact bricks and classify them as façade objects but at the same time to highlight the potential damage between the bricks and also through them. Moreover, a value of 15 in the spectral difference segmentation algorithm was enough to merge similar areas and keep the potential damage features intact. It is clear that those segmentation parameters have to be adjusted for different materials as they are strongly related with the geometrical and spectral properties of the surface on which the crack may appear. However, per material could be possible to adapt a narrow range of values.

In Figure 29 in the left image, the result of the multiresolution step is illustrated. As it can be seen the resulted image in the current step is over-segmented with many small segmented objects. However, with the spectral difference segmentation step the façade is represented by meaningful objects in terms of highlighting the damage features (Figure 29 right image).

Figure 29. MLS segmentation on the "Brick II" (no flash) (left) and spectral difference segmentation result (right).

2. **Classification**

The same classification approach as in the concrete ruleset was followed in the "brick" samples. First, an initial classification procedure between potential damage features and façade was performed based on the brightness value (>299) of the layers and a DSM value of less than 999. In Figure 30 in the left image, the binary result between potential damage (yellow colour) and the rest of the background/façade (grey colour) can be seen. The brick is more complex case than the concrete as they in between mortar joints among the bricks can be misclassified as cracks if the classification parameters will not be carefully selected. In order to eliminate small artefacts that were classified as potential damage, a refinement process was applied where objects with area less than 470 pixels were classified as façade.

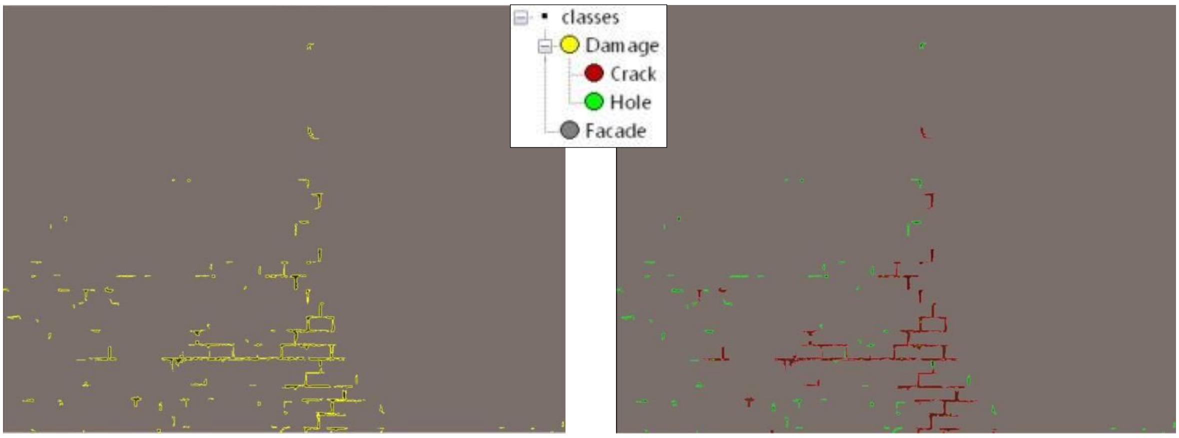

Figure 30. On the left an example of the binary result between "damage" and "façade" on "brick II" (no flash) sample area. On the right, the resulted classification in cracks and holes.

For this case the threshold of the number of pixels was selected by comparison with the smallest crack on the facade. The latter one was prior knowledge. In a real case scenario this threshold could be indicated from the experts based on the minimum damage feature size that is considered as meaningless.

The last step of the classification process was to provide a final characterization of the potential damage objects as cracking or hole features (Figure 30 right image). First, all the damage features were assigned as cracking features by assuming that all the damage features are cracks. Next, objects with area less than 2500 pixels and rectangular fit more than 0.5 were categorized as holes. In the end a final merging of the created classes were carried out to merge similar neighbouring classes.

In Figure 31 the result of the final classification of the "brick II" is illustrated but with the use of the flash light. The result demonstrates that some parts of the crack on the middle part of the image have not been detected. Even if the flash image-based DSM included more details than the one with no flash, the classification result was not as it was expected.

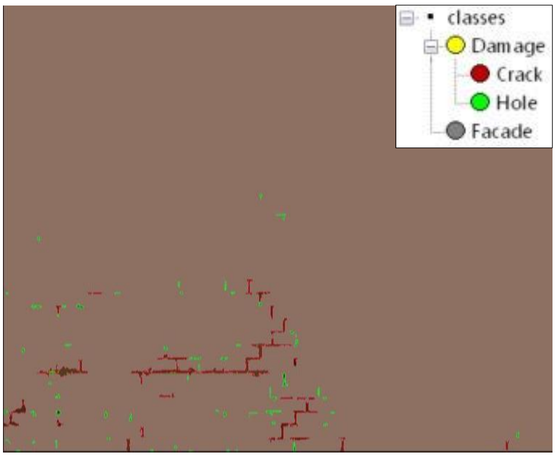

Figure 31. Result of the classification in "brick II" with the flash light

"Brick I"

The same approach was attempted in the damage sample "brick I" by applying the same ruleset with no success (Figure 32). In the left image the resulted classification on the sample area "brick I" with the flash light produced solely one object classified as façade. In the right image the results of the classification from the dataset under the ambient light. It can be seen that in both samples the ruleset did not work properly in order to extract the damage features of interest (cracks and holes). The current sample was the first dataset that was acquired and produced and it includes a hairline crack of maximum width of 1.2 cm.

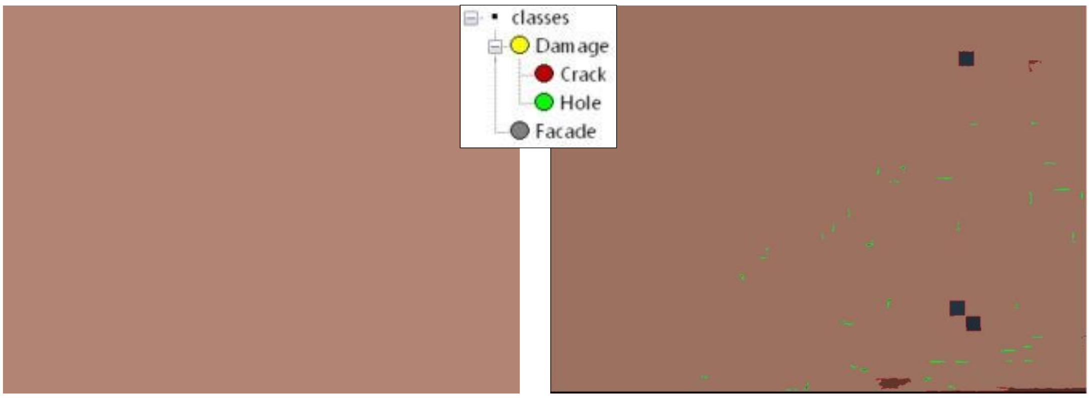

Figure 32. Classification result of "brick I" with flash light (left) and with no use of flash (right).

This is the first case that the hybrid approach did not return any damage feature. That gives an indication related with the size of the crack that can be detected from this ruleset. The case of Brick II was crack of maximum width of 2.5 cm while the current hairline-crack of 1.2 cm. The first one was recognizable but the latter no.

For the current experiment in the damage sample “brick I”, two extra classification ruleset were designed one for the flash and one for the no flash dataset based on the existing brick ruleset but with some modifications in object’s characteristics values. In Figure 33 the updated results of the classification are illustrated. It can be seen in Figure 33 that the enhanced rulesets were produced better results on the current sample than the previous one but a lot of noise and artefacts are included in the results.

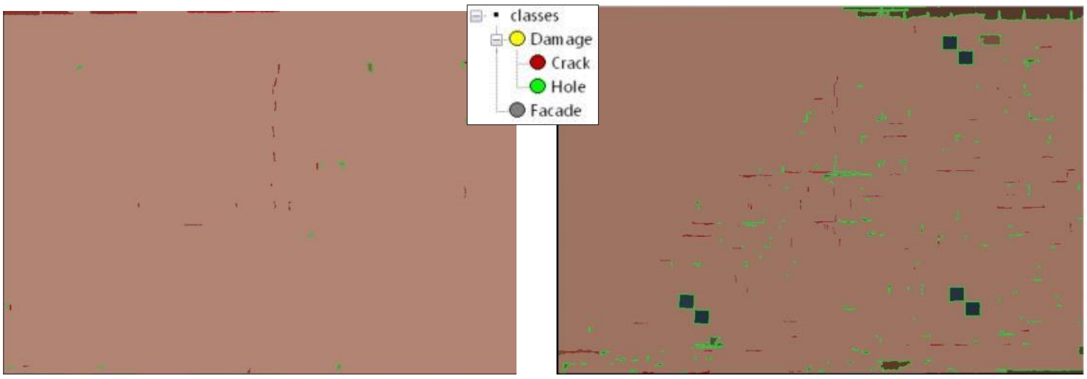

Figure 33. Result of the updated classification in “brick I” with the flash light (left) and with no use of flash (right).

After this conclusion there was tested if different parameters for the height and brightness threshold could give a better result. This test classified small parts of the damage feature but the result was not complete.

4.3.2.3. Insulating material

All the insulating samples were analysed with the same designed approach. As a consequence the same ruleset was developed and applied in both the flash and no flash sample. The damage elements that were attempted to be identified are holes and cracks, same approach as in the previous samples. The current damage sample found to have the simplest damage pattern as a result the feature extraction had the highest thematic accuracy.

1. **Segmentation**

Following the same approach as before, a multiresolution segmentation algorithm (Table 11) was performed to segment the imagery in meaningful objects in combination with a spectral difference segmentation algorithm to merge similar segments based on their mean intensity values.

Algorithm	Parameter	Value
Multiresolution segmentation	Scale	100
	Shape	0.8
	Compactness	0.5
Spectral difference segmentation	Spectral difference	20

Table 11. Segmentation parameters for insulating material

The selected compactness and shape parameters for the ITC “insulating material” were high in comparison with the ones for the concrete and brick samples. This is due to simpler damage pattern with a large background and elements that do not fit in their environment. A value of 20 was enough for the spectral difference segmentation step in order to merge similar objects and keep the ones that are valuable for the classification process.

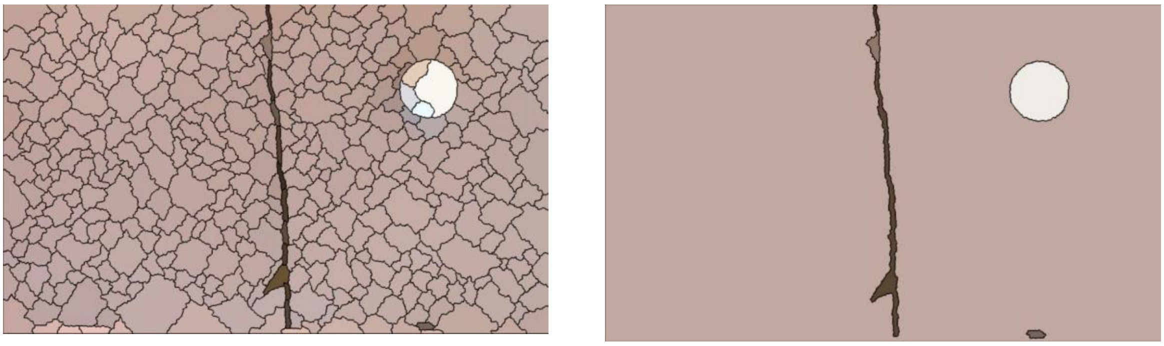

Figure 34. On the left an example of the multiresolution segmentation on the "insulating" sample (no flash). On the right the result of spectral difference segmentation on the result of multiresolution segmentation

In Figure 34, the result of the multiresolution segmentation step in the damage sample of the insulating material with no use of the flash light is illustrated in the left image. It can be highlighted in the current step the over segmentation of homogeneous objects such as the background material. In the right image, the spectral difference segmentation step was adequate to merge similar objects but keep as individual objects the ones that do not fit in with the rest.

2. **Classification**

The classification process in the insulating material followed the same approach as the previous damage samples. First a binary classification between potential damage features and façade was processed based on the brightness value and the DSM values. In addition an extra object characteristic (area) was used in the current step in order to provide a more accurate initial classification. In Figure 35 the binary result between damage and façade is illustrated. As it can be seen in the figure, the image is constituted from a large area as background where it is the classified façade and some features that are highlighted with yellow colour which is the potential damage features.

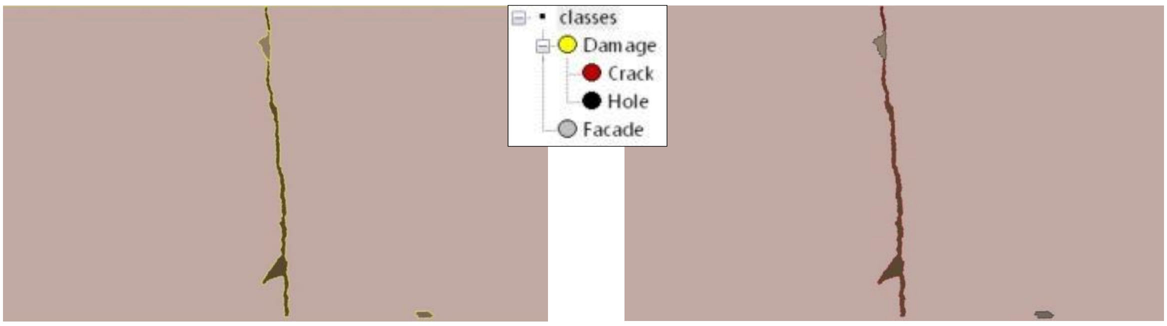

Figure 35. On the left an example of the binary result between "damage" and "façade" on "insulating material" with no flash usage. On the right, the resulted classification in cracks and holes.

The last step of the classification process was to characterize the damage features as cracks or holes. More specific, the objects' characteristics such as ratio length/width and rectangular fit were used to further classify the objects in one of the categories explained before. Objects that had a ratio length/ width value of more than 5 and a rectangular fit value of 0.5 and less were classified as cracks and the rest as holes.

The same developed ruleset was implemented for the flash dataset of the insulating sample. In Figure 36 the result of the classification in the insulating material with the flash light is illustrated. It can be noticed that the flash result includes one element which is classified as crack feature in comparison with the no flash dataset where the current object was divided in two parts classified as cracking features and a small part in the middle classified as hole. In the reference data, the elongated damage element is digitized as one continuous crack and there is the presence of a small hole in the image at the down part.

Figure 36. Result of the classification in "insulating material" with the use of flash light.

After the feature extraction the current crack on the insulating material was exported in a vector layer in combination with its geometrical properties (area, length and width) as eCognition calculated them. More specific, the length was 1479pixels and the width 134.5 pixels. These numbers with a pixel size of 0.03 in the current samples are translated as follow:

Length: 1479.14 * 0.03 = 44.374cm (**Reference length** = 57cm)

Width: 134.5 * 0.03 = 4.035cm (**Reference width** = 4.1cm)

The resulted geometrical properties were computed automatic from OBIA software. The concept of the calculation of the width and length in this eCognition software is carried out by using the ratio of length to width derived from the minimum bounding box approximation. As a result the properties of length and width are not the actual sizes of the feature but an approximation based on the ratio length to width.

4.4. Accuracy assessment

Two different methods are applied for the procedure of the accuracy assessment. The first approach follows area based measurements, once developed in R environment to be more automated and also in ArcGIS. Second, a point based approach based on individual measurements of points to define properties such as the total length of the crack is presented.

4.4.1. Area based approach

The outcome of the accuracy assessment of the extracted damage features is presented in Table 12. As stated before, the accuracy assessment was based on a reference dataset created by manual digitization of visible damage feature including holes and cracks in ArcGIS. The reference data was overlaid with the result of the classification in OBIA. A more detailed illustration of the classification quality and errors can be found in appendix 7.5 where the factors of TP, FP and FN are overlaid on the imagery as green, red and yellow areas respectively.

	Brick I		Brick II		Concrete I		Concrete II		Insulating material	
Flash	TP	24.2 %	TP	36.2 %	TP	23.6 %	TP	5.3 %	TP	91.1 %
	FP	24.4 %	FP	28.0 %	FP	40.9 %	FP	74.5 %	FP	5.6 %
	FN	51.4 %	FN	35.8 %	FN	35.5 %	FN	20.3 %	FN	3.3 %
	Split factor	1.0	Split factor	1.3	Split factor	0.6	Split factor	0.1	Split factor	16.1
	Missing factor	2.1	Missing factor	1.0	Missing factor	1.5	Missing factor	3.84	Missing factor	0.04
	Correctness	49.7 %	Correctness	56.3 %	Correctness	36.6 %	Correctness	6.6 %	Correctness	94.2 %
	Completeness	31.9 %	Completeness	50.2 %	Completeness	39.9 %	Completeness	20.7 %	Completeness	96.5 %
No flash	TP	17.8 %	TP	44.8 %	TP	66.5 %	TP	25.2 %	TP	78.4 %
	FP	10.1 %	FP	31.0 %	FP	29.3 %	FP	73.0 %	FP	4.3 %
	FN	72.0 %	FN	24.2 %	FN	4.2 %	FN	1.7 %	FN	17.4 %
	Split factor	1.8	Split factor	1.4	Split factor	2.3	Split factor	0.3	Split factor	18.3
	Missing factor	4.0	Missing factor	0.5	Missing factor	0.06	Missing factor	0.07	Missing factor	0.22
	Correctness	63.8 %	Correctness	59.1 %	Correctness	69.4 %	Correctness	25.7 %	Correctness	94.8 %
	Completeness	19.8 %	Completeness	65.0 %	Completeness	94.1 %	Completeness	93.6 %	Completeness	81.9 %

Table 12. Summary of the accuracy assessment

From Table 12 can be seen that the split factor was high for all the images except the "concrete I" (flash) sample and the "concrete II" (no flash). In the rest of the images the factor has a high value with a highlight in the insulating material.

The missing factor was fluctuated in low values for the samples with no use of the flash light except "brick" which produced drawbacks in OBIA step. However for the flash datasets the factor is close to 1 and in some cases it exceeds 1. The "insulating material" solely showed low values of missing information in both illumination scenarios.

The correctness factor which is represented in percentage (%) seems to have moderate results with a medium value around 60% for all samples except the insulating samples where the correctness factor reaches a peak around 94%. The latter demonstrates that a critical amount of damage information was not correlated accurately with the reference damage dataset. For the completeness factor the medium value is fluctuating in higher values around 80%. If the sample "brick I" is excluded which was problematic the only sample that had low completeness factor was "concrete I" with the use of flash light where a lot of surface artefacts where classified as damage features.

Then using the R script the true positives were calculated for the sample "insulating material". That was done in order to assess the difference between the results of no buffer around the reference data and a buffer of 5mm. The result was the expected, meaning that the TP value that was calculated with the buffered reference was higher than the case without a buffer. Specifically, for the insulating material – no flash case the TP without buffer around the reference data was 78.4% while for the buffered case it was 97.8%. This is because all the pixels relatively close to the border of the reference, no more than a pixel, were now classified as damage. (Figure 37) In blue colour the areas that are correlated as potential damage features are presented. In addition, in green colour are illustrated the areas that were identified as damage features in the reference but it did have not been extracted as damage features in OBIA result. In appendix 7.3 the developed script is demonstrated in details.

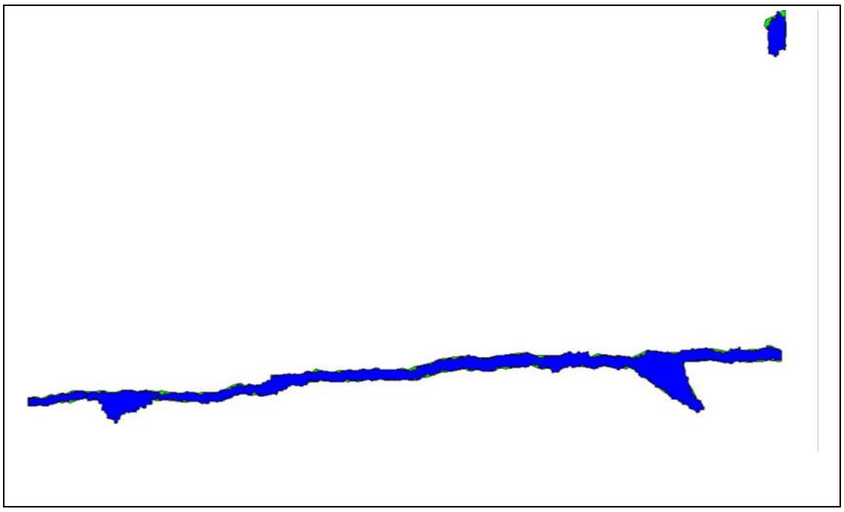

Figure 37. Result of the accuracy assessment at the “insulating material” in R environment. Blue: Validated damage feature, Green: Unidentified damage feature

In addition, the results of the classification of Galarreta’s ruleset were tested with the same script in R for the case of the brick II with flash (Figure 38). The difference between the results of the two rulesets is significant (Table 13).

Brick II - flash	TP (R – project (5 mm buffer zone))		TP (ArcGIS (no buffer))
	Galarreta (2014)	TP (Current ruleset)	TP (Current ruleset)
	2 %	48 %	36.2 %

Table 13: Comparison of TP between the result of Galarreta ruleset and the current for the Brick II (with flash) case.

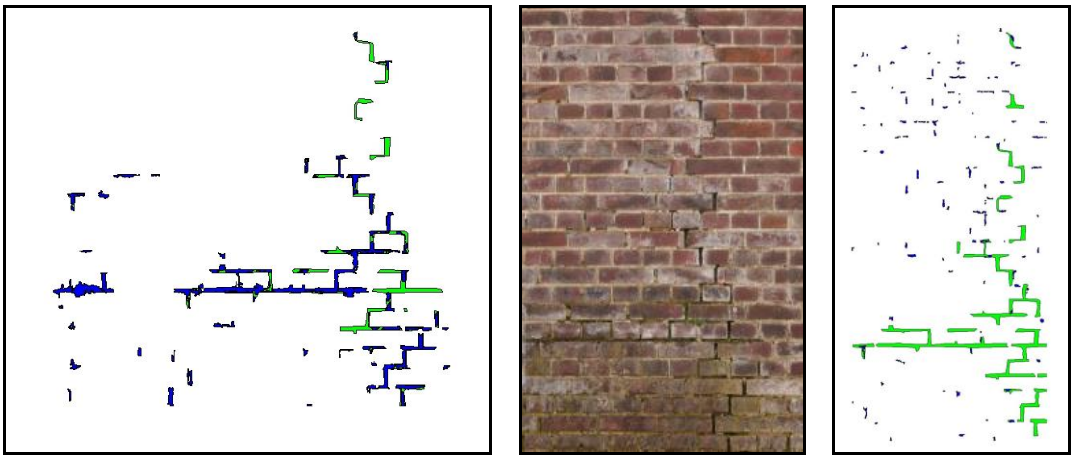

Figure 38. Result of accuracy assessment of current (left) and Galarreta's ruleset (right) on sample "brick II" flash. In green the areas that were not identified and in blue those who were TP.

4.4.2. Point based approach on LiDAR data

In order to create a validation dataset for point measurements of the acquired damage features a laser scan was performed on the “insulating material”. The laser point cloud was co-registered with the resulted image based point cloud in order to visualize any potential differences between the two clouds (Appendix 7.6). In Figure 39 the result of the registration is illustrated from a vertical and horizontal perspective respectively. The resulted mean difference between the two clouds was less than 0.2 mm which is a negligible difference between the two clouds as a result the crack region was registered without any systematic problems. However the inner part of the crack and more specific its inner geometry had been identified solely from the laser scanner but was not presented in the image based cloud where the mentioned areas were presented as occluded areas.

Figure 39. The crack area of the registered point clouds.

First, manual measurements were carried out on the "insulating" sample in order to find out the real length or in other words the distance between the start and the end point of the crack. It has to be pointed out that in order to avoid errors during the measurement process with the ruler the distance between the start and the end point was measured 10 times. The total length was calculated as the straight line from the start point of the cracking area until the end. The distance was calculated 0.57m. In Figure 40 the cross-section of the crack in the laser point cloud.

In the current experiment, in order to validate the length parameter of the current crack and at the same time to strengthen the statistical measurement and reliability, 10 different users have been asked to define the start and the end points of the crack region by providing in prior a short definition of what is defined in the current thesis as a crack feature. Under this research the assumption which has been made in order to proceed with the validation is that the crack length is represented by the distance between the two visible end points. In reality the crack length is defined as the length of its middle points or its skeleton. Moreover the roughness layer of the registered point cloud was calculated in order to enhance users' interpretation capability. Each of the users delivered two points with the relative coordinates (x_1, y_1, z_1, x_2, y_2, z_2) and the resulted distance – length. Next, the average length of the 10 measurements was calculated in order to exploit the length that was resulted from the users' perception. The obtained average length was 0.578m which is real close measurement to the one that was calculated with the ruler in situ. It could be concluded in the laser experiment that the current data provided enough information to the users to interpret the feature of interest accurately and produce a strong correlation between the two measurements.

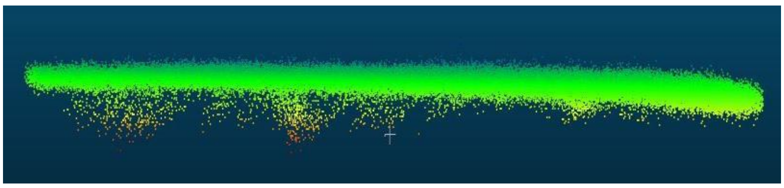

Figure 40. Cross-section of the crack region (laser point cloud)

5. DISCUSSION

The aim of the current chapter is to explain in details the limitations and drawbacks have been found in relation with the input data, the proposed methodology and the obtained results. In addition, a detailed description of the conflictive points that came across is provided.

5.1. Image acquisition

It was clear that the step of image acquisition is critical in order to collect all the appropriate imagery to proceed to the generation of the DSM and orthophoto. Limitations such as difficulties to collect the data due to inaccessible sites could have been overcome with the use of a UAV platform. However, the challenges of using the latter are the weather conditions and an expert with certificate to fly the airborne platform. However, the focal length of the sensor should be carefully selected and the GPS system on the UAV platform should exist to provide initial approximations.

In addition, the minimum detectable crack size proved to be a crucial parameter for the proposed study, as an undetected cracking feature may be the subject of future degradation. This study found that even the hairline cracks (<1cm) could be detected but not quantified due to the limited visibility of their geometrical properties on the imagery. In contrary with cracks more than 2cm in width where parts of the crack interior were visible. Although cracks in brick buildings were much more easily discerned than those in concrete ones. Thus before the image acquisition the minimum size of the crack that needs to be identifiable should be known and the flight mission should be based on that.

A serious drawback that has been found in the current research is the dependency between sensor viewing angle and crack geometry (Figure 41a). The position and the viewing angle of the sensor during the image acquisition proved crucial in order to collect all the available information of the crack geometry. A valuable parameter that could be obtained from the crack geometry is its depth. When the damage on the façade is represented by hairline cracks with less than 1cm the inner part of the crack is not visible from the sensor (Figure 41a). In simple cases where the crack is constituted by a simple 'U' morphology the depth acquisition is possible if the sensor's viewing angle is the same with the depth direction of the crack (Figure 41b).

However, in more complex cases, that are more close to real case scenarios the crack internal geometry could be complex (Figure 41c) and the actual depth of the crack is not able to be captured. In cases such as the latter where there are parts of the crack that are occluded and no information is available the crack depth is not able to be obtained with reliability. In Figure 41d the crack region is fully opened as a result the sensor is capable to obtain information of the actual depth due to that the sensor beams are able to reach the actual depth of the crack. In traditional surveys made in situ, the depth acquisition is performed with a thin measure tape or a ruler. The expert is putting a "measure tape" inside the crack region till it finds an obstacle in the structure and measure the depth of the point. Again the latter does not constitute a reliable and accurate measure to acquire crack depth information due to the crack complex geometry.

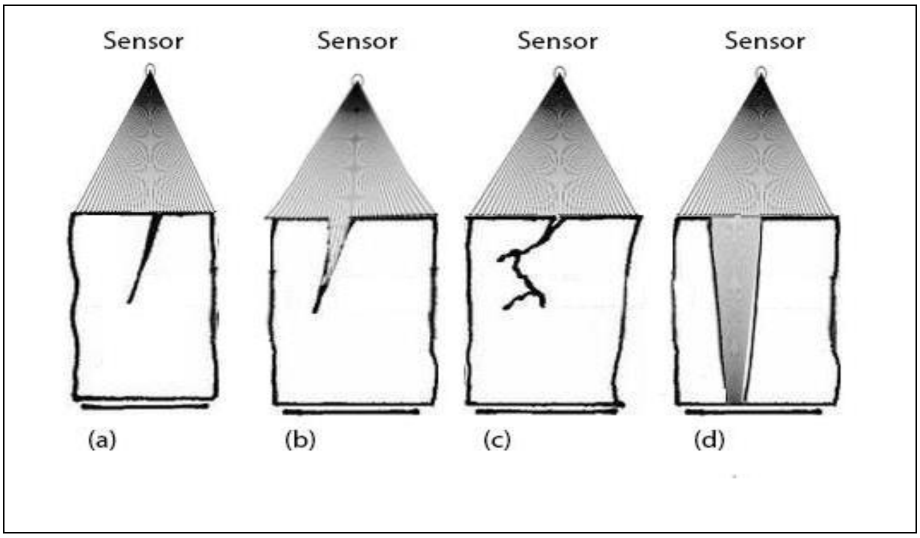

Figure 41. Crack geometry – Sensor viewing angle

5.2. Photogrammetric data

In Pix4D software the two products, DSM and orthophoto were generated based on the collected imagery. The computational time was in accordance with the number of photos and the resolution of the imagery. After multiple experiments on the number of images that are adequate to generate the two products with high reliability a number of 17-27 images found to be efficient. However the current choice was based on the size of the sample areas that were investigated in the current research and the image acquisition set up. In general, the number of images is in direct relation with the area coverage and also in relation with the spatial resolution of the images. In the current experiment, the computational time to produce the outputs from the selected imagery was approximately 14-18 minutes. In samples such as ITC "insulating" material where the area coverage was smaller than the rest of the samples the computational time was around 8-10 minutes. In the end, the resulted products were reliable enough to use them in the next step of image analysis. However, in some cases such as in "concrete II" and "brick I" the resulted DSM in the no flash dataset was derived with noise (appendix 7.2). After the results, it could be concluded that the use of a flash light is augmenting the identification of façade's elements and it is capable to highlight small details that are not visible under the ambient light. On the other side, the enhanced illumination modifies the brightness values of the pixels.

Another significant observation made from the results in the current thesis was that in most of the damaged samples where there is a presence of crack the two sides, left and right of the opening of the crack are on different level. That affects the height threshold at the classification step and can cause issues especially for the detection of the hairline cracks where the depth is really small. In Figure 42, a cross-section in a part of the cracked region on the brick II where the shift between the crack regions is visible. It seems that there is a relation between the small elevation differences and the depth of the crack. It is an interesting fact that came out from the results and it could be added for further investigation in the future research.

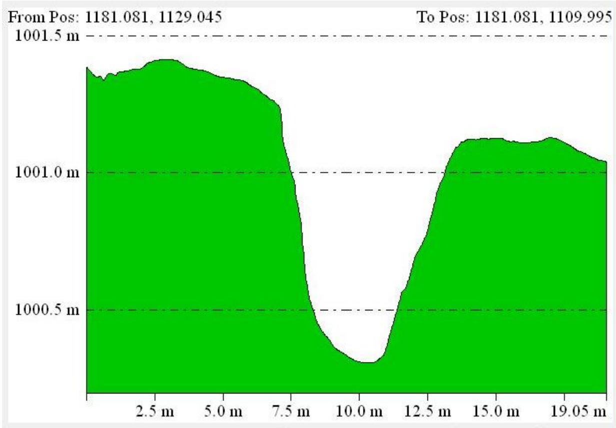

Figure 42 Height difference between the two sides of the crack "brick II".

5.3. OBIA

5.3.1. Galarreta's OBIA rulesets

At first the developed rulesets from Galarreta's research were adapted and implemented for the damage samples in the current thesis. Due to the fact that the former's rulesets designed only for RGB imagery, the orthorectified image was used to process that step. The results showed that the adapted rulesets were not able to identify and classify the damage features accordingly. The cause of the misclassification begins with the different classes that are created to serve the imagery in accordance with the different input data. Also, that ruleset was designed mostly on the geometrical characteristics of the object and was not based on the current assumption. Here the segmentation was also based on the assumption that the damage areas have low brightness because of the shadows. The latter is influenced significantly from the selected segmentation parameters which are based in the current research on the 2.5D DSM and the brightness value of the cracks and holes on the orthoimage. This information in combination with the height properties of the damage areas in relation with the main plane (façade) height could lead to the identification of the damage features.

5.3.2. OBIA analysis

The damage features like holes and cracks which were extracted by OBIA techniques were found reliable and representative of the damage that was identified on the sample areas as initial signs of deterioration. It is important to notice that a more detailed damage catalogue could be more effective. From the selected features, the main focus of this research was initially focused only on the cracking features but after careful consideration features such as holes were included in the features that had to be extracted. The latter was based on the assumption that holes could be the initial point where a crack could propagate from.

- **Damage feature extraction**

At first, it has to be noticed that there are a lot of different segmentation and classification approaches which a user can apply to proceed with the damage extraction from building facades. In the current thesis a coherent image-based approach was developed based on extended literature review and discussions with experts. The OBIA methodology was based in the assumptions posed in methodology chapter where the damage features are represented in the data from pixels of low brightness and less elevated captivities.

Three distinct rulesets were developed in the initial stage to capture the damage features for the three different materials that were under investigation (concrete, brick and insulating material). Different materials have different spectral properties and because of that, parameters like the threshold of brightness had to be adjusted. Apart from that, the three materials because of the different texture gave different segmentation results; especially, for the case of the brick. There, an additional rule should be added in the set in order to refine the result.

First, the image of each case was segmented in homogenous objects based on a combination of segmentation algorithms followed by the classification process (chapter 4).

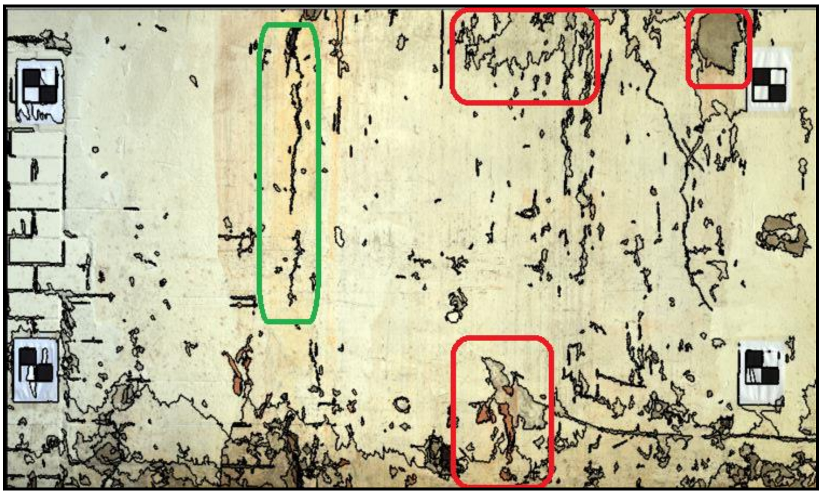

Figure 43. In the green area the actual cracks "concrete I". In the red areas objects that were wrongly highlighted as independent objects after the segmentation process.

In addition, the selected damage classes have proved to be sufficient for the appropriate classification process under the experiments that carried out in this thesis. The damage samples did not include any non-structural features such as windows or doors and such no semantics were included in the rulesets.

a) Segmentation

All the damaged samples were analyzed with the same segmentation approach. First, a multiresolution segmentation process was applied in the samples to highlight the damage features of interest, followed by a spectral difference segmentation process where similar objects were merged based on their mean layer intensity values. Despite that the selected approach captured damage features of cracks and holes in the imagery, in some cases the background elements were wrongly highlighted as objects of interest. Especially, in the case of concrete where the sample area was complex many features such as decorations on the wall or plaster removal that were categorized as damage. In order to be able to include even the small thin cracks on the façade, the developed segmentation ruleset included also features that had dark color due to the illumination conditions and the produced occluded areas. Later with the designed classification parameters the segmented artefacts were included as façade objects.

In Figure 43 the result of the segmentation process in the sample "concrete I" is illustrated. In red rectangular boxes are presented the areas that are wrongly segmented as objects and are distinguished from the rest of the background due to their brightness values. In the green box the actual cracking feature that was identified during the field visit.

b) Classification

The aim of the classification step was to assign meaningful classes at the objects that were resulted from the segmentation process. The developed rulesets were able to identify a significant part of the damage features in most of the samples with high reliability. However, in some complex cases the resulted classification failed to detect even the visible damages with the current set of ruleset. The classification process was based on two major assumptions in the current thesis. The 2.5D DSM would provide elevation information of the damaged façade and the orthorectified image should provide the brightness information. As a result, in some cases where the obtained DSM had noise, the results from the image analysis step showed errors. For instance, in the sample of "Concrete II" one extra classification rulesets had to be designed in order to fulfil the requirement of a comprehensive classification. In addition, the DSM had different values between the flash and the no flash especially for the concrete and the brick. The latter is due to the fact that the flash light is augmenting the brightness values of the projected layers. This results in errors in OBIA process due to the modified parameters of the objects. Consequently, the developed set of classification rules on the flash dataset was not capable to be applied directly on the no flash dataset. Moreover, in the sample of "brick I" where a small hairline crack was present the developed ruleset for brick materials was not capable to extract the cracking feature due to its small size and also the current crack was not visible on the DSM as damage element.

Due to high complexity in some of the damage samples, the classification process had been included some background objects wrongly. In Figure 44 the result of the classification in the damage sample of "concrete II" is illustrated. As it can be seen the crack that exists in the upper left part of the image was identified reliably in the classification process. However, there are multiple small objects that were classified as holes. As it can be seen in the real photo, the current façade includes a rectangular box where the two targets are also attached. The rectangular box is window which was used to allow the transition of the air in the interior of the building. As a result the small holes that it is constituted the box are classified as potential damage features and more specific as holes. In reality the current box is constituted from small holes but they are not signs of damage. Also, a small part of the attached GCPs is classified with the rest artefacts as holes.

Figure 44. In the green area the actual cracks on the damage sample "concrete II". In the red areas objects that were wrongly highlighted as independent objects after the segmentation process. At the down left part, the façade as it is in reality.

5.4. Accuracy assessment

The accuracy assessment procedure was carried out with two different approaches based on spatial logic operations. First an area based approach was proceed divided in two sub steps, one with the Union operation in ArcGIS in order to calculate the TP and FP that are then used for the completeness correctness assessment. Similar approach was executed via a script in R-project to calculate the TP in a more automated way. This time a buffer zone of a pixel was included. That increased the accuracy. The aim of both procedures was to compare the area between the extracted objects from OBIA with the digitized reference data. Several statistical measurements were done to assess the quality of the classification. They are explained in details in chapter 4.

Secondly, a point based approach was followed based on the use of the laser point cloud that was acquired from the indoor experiment in ITC building. Based on the measured length on the point cloud by 10 different users in exchange of a strong statistical measurement, the average length measurement was obtained and compared with the one that was measured manually in situ. The outcome of the average given distances has been found the same with the one measured manually (0.57m). After the result it could be concluded the TLS point cloud could constitute another reliable data for the identification of the damage features and their geometrical properties.

5.5. Current research as a real case application

As it was discussed earlier, the current research could be directly linked with the real case application of structural damaged assessment in the area of Groningen by TNO. As one of the stages in TNO's SDA is to assess the damage based on single imagery, our research could be a promising method to augment the efficiency and effectivity of current applications. In order to use a single post-event imagery, an acquisition of 12-17 VHR overlapped images could be efficient to detect and extract valuable damage information. This is more than a change detection method of identifying the damage fissures and more specified the cracking features. This will constitute extra information for the structural experts to assess the structural integrity more reliably.

What should be carefully considered for the TNO case is the different construction materials that are present in their study area. This research proved that different material need to be dealt with different parameters and thus no unique approach could lead to a result. Also, the use of the DSM can give enhance the result and come to the identification and characterization of the damage features. The accuracy in terms of completeness and correctness is not yet high for all the materials but further study could improve that.

6. CONCLUSION & RECOMMENDATIONS

6.1. Conclusion

This study aimed to produce a methodological framework that can be used for comprehensive damage characterization of surface cracking features using image based techniques on VHR imagery. The current approach was explored by using a terrestrial platform with a VHR sensor mounted on it for the image acquisition step. The same workflow for damage characterization could be carried out with the use of an airborne platform and specifically a UAV in order to proceed with the data acquisition efficiently in a manner of time and cost. The conclusion of the study is that based on the literature review there ws need for a new framework to provide accurate and reliable information for the damage feature on constructions. Thus it was decided to explore if the image based analysis in OBIA on VHR imagery could provide any such possibility. For that different materials were tested to assess how same objects behave in different material. Also, per material the case of ambient illumination and enhance from additional source were explored.

The conclusion is that the several types of crack in terms of geometrical characteristics and environment (material) need different ruleset to be characterised. There were cases that the crack was successfully identified and characterised but that was only there were the texture of the material was simple and smooth, the geometry was also planar. The more complicated like the brick did give the same level of high accuracy. For these cases further study is required.

The main conclusion after all is that the assumption that the damage features have lower brightness values in the orthorectified image and are located in lower height than the mean height of the façade contributed at a high level. Also,the images with the additional illumination did not give the expected results. The accuracy from these images were much lower for the more complex cases (e.g. brick).

The answers for the research questions are:

1. **What are the crack related categories that already have been studied?** The crack related categories are presented in Table 1 where different cracking patterns are illustrated on brick and concrete material. This was the initial reference data in order to get to know the damage elements that will come across on the materials under investigation.
2. **What are the "to be produced" data from the acquired imagery in order to identify the features of interest?** Two were the outputs that had "to be produced" from the acquired imagery. The DSM which constitutes a 2.5D with the elevation of the façade and all he objects close to it and the orthorectified image.
3. **How to segment the images in order to extract accurately the damage features of interest from the sample areas?** The choice of combining the multiresolution segmentation with the spectral difference segmentation gave segmentation results from all the available segmentation processes in OBIA. The selected approach with different parameters for each material returned damage features but not of very hogh accuracy per case. Further study is required to improve the result.
4. **What are the most important crack's geometrical properties and which of them can be extracted by using image-based techniques?** After careful consideration and the geometrical properties that could be extracted in relation with the highlighted objects were the length, the width and the area of the extracted damage features.

5. **Which information can be used to extract the features of interest by Object-Based Image Analysis (OBIA)?** Based on the assumption that the damage features have predefined geometrical properties like cracks are elongated fissures and holes have a circular or rectangular shape, a set of object's characteristics such as the ratio length to width, rectangular fit and the area were used to extract the cracking features and holes. Also the assumption that the crack damage features have lower brightness values in the orthorectified image and are located in lower height than the mean height of the façade contributed at a high level.
6. **Can additional active illumination source enhance the crack result?** From the resulted DSMs and orthophotos it can be concluded that the use of a flash light to illuminate the area of interest has be proved to produce detailed results especially for the resulted DSMs in contrary with the no flash datasets. However on the image analysis steps the use of a flash light was producing higher brightness values than without which resulted in some modifications in the classification steps.
7. **What is the geometric accuracy of the extracted features characteristics?** The geometric accuracy is of ±5mm and the accuracy of the proposed methodology is different for each material and is given in Table 12.

6.2. Recommendations

The recommendations for future research are:

1. The stage of image acquisition could be transformed in a robust and automated approach by using a UAV platform to gather the appropriate imagery for further damage characterization. Especially for elevated infrastructure where the damage features are not visible from the ground a UAV platform should be ideal to perform a predefined flight path around the targeted building.
2. The collection of more damaged facades and cases that are presented more complex in order to augment the applicability of the current methodology in other scenarios.
3. Enhance the OBIA process by adding more child classes for the damage feature such as crack category based on selected attribute. In addition, more "in deep" choice of the objects' characteristics could be proved more accurate for the classification process.
4. From the discussion with the experts, essential information for damage assessment is the depth of the crack and its relation with the width. As the limitations of the imagery to present areas that are not visible, a future research on how can the depth information can be derived with the use of the point cloud in combination with a laser point cloud could be effective.
5. The stage of the accuracy assessment with the laser sensor could be transformed in an automated way in order to derive geometrical information such as the area of the crack, its length and maximum width. In a brief literature review a watershed segmentation of the point cloud could be applied and test the results in a future research.
6. In addition, the developed script in R-project could be enhanced with a set of commands to produce further statistical measurements for the examined areas.
7. The assumptions based on which the current research was done (brightness and relative position of the crack in relation with the façade plane) can be used to develop further the rulesets and combine them with the ruleset from Galarreta. The combination of the two approaches is expected to lead to results of higher accuracy at a building level. Then the severity can be also estimated.

LIST OF REFERENCE

Abdel-Qader, I., Abudayyeh, O., & Kelly, M. E. (2003). Analysis of Edge-Detection Techniques for Crack Identification in Bridges. *Journal of Computing in Civil Engineering*, *17*(4), 255–263. doi:10.1061/(ASCE)0887-3801(2003)17:4(255)

Abdel-Qader, I., Pashaie-Rad, S., Abudayyeh, O., & Yehia, S. (2006). PCA-Based algorithm for unsupervised bridge crack detection. *Advances in Engineering Software*, *37*(12), 771–778. doi:10.1016/j.advengsoft.2006.06.002

Abudayyeh, O., Al Bataineh, M., & Abdel-Qader, I. (2004). An imaging data model for concrete bridge inspection. *Advances in Engineering Software*, *35*(8-9), 473–480. doi:10.1016/j.advengsoft.2004.06.010

ACI Committee 224. Causes Evaluation and Repair of Cracks in Concrete Structures, 1 masterbuilder.co.in (2007). Retrieved from http://www.masterbuilder.co.in/data/edata/Newsletter/V4N2/88.pdf

Adhikari, R. S., Moselhi, O., & Bagchi, A. (2014). Image-based retrieval of concrete crack properties for bridge inspection. *Automation in Construction*, *39*, 180–194. doi:10.1016/j.autcon.2013.06.011

Aibotix. (2014). Aibotix. Retrieved January 01, 2014, from https://www.aibotix.com

Amarasiri, S., Gunaratne, M., & Sarkar, S. (2010). Modeling of Crack Depths in Digital Images of Concrete Pavements Using Optical Reflection Properties. *Journal of Transportation Engineering*, *136*(6), 489–499. doi:10.1061/(ASCE)TE.1943-5436.0000095

American Concrete Institute. (2011). *ACI 318-11: Building Code Requirements for Structural Concrete and Commentary* (First Edit., p. 503).

Applied Technology Council. (2005). *ATC-20-1 Field Manual: Postearthquake Safety Evaluation of Building* (p. 159). ATC,.

Arias, I., & Achenbach, J. (2004). A model for the ultrasonic detection of surface-breaking cracks by the scanning laser source technique. *Wave Motion*. Retrieved from http://www.sciencedirect.com/science/article/pii/S0165212503000908

Asnaashari, E., & Sinha, J. K. (2014). Crack detection in structures using deviation from normal distribution of measured vibration responses. *Journal of Sound and Vibration*, *333*(18), 4139–4151. doi:10.1016/j.jsv.2014.04.057

Bell Laboratories. (2014). R Studio. Retrieved from http://www.r-project.org/

Blaschke, T. (2010). Object based image analysis for remote sensing. *ISPRS Journal of Photogrammetry and Remote Sensing*, *65*(1), 2–16. doi:10.1016/j.isprsjprs.2009.06.004

Blaschke, T., Lang, S., & Hay, G. (2008). *Object-Based Image Analysis: Spatial Concepts for Knowledge-Driven Remote Sensing Applications* (2008th ed., p. 817). Springer; 2008 edition.

Blaschke, T., & Strobl, J. (2001). What's wrong with pixels? Some recent developments interfacing remote sensing and GIS. *GeoBIT/GIS*. Retrieved from http://scholar.google.com/scholar?hl=en&btnG=Search&q=intitle:What+'+s+wrong+with+pixels+?+Some+recent+developments+interfacing+remote+sensing+and+GIS#0

Bloch, H., & Geitner, F. (2012). *Machinery Failure Analysis and Troubleshooting* (p. 760). Butterworth-Heinemann.

Burland, J. B., Broms, B. B., & De Mello, V. F. B. (1977). Behaviour of foundations and structures: State of the Art Report. In *Proceedings 9th International Conference on Soil Mechanic and Foundoution Engineering Session II*. Tokyo.

Chen, L.-C., Shao, Y.-C., Jan, H.-H., Huang, C.-W., & Tien, Y.-M. (2006). Measuring System for Cracks in Concrete Using Multitemporal Images. *Journal of Surveying Engineering*, *132*(2), 77–82. doi:10.1061/(ASCE)0733-9453(2006)132:2(77)

Chen, S.-E., Rice, C., Boyle, C., & Hauser, E. (2011). Small-Format Aerial Photography for Highway-Bridge Monitoring. *Journal of Performance of Constructed Facilities*, *25*(2), 105–112. doi:10.1061/(ASCE)CF.1943-5509.0000145

Danielgm. (2014). CloudCompare. Retrieved October 08, 2014, from http://www.danielgm.net/cc/

Dell'Acqua, F., & Gamba, P. (2012). Remote Sensing and Earthquake Damage Assessment: Experiences, Limits, and Perspectives. *Proceedings of the IEEE*, *100*(10), 2876–2890. doi:10.1109/JPROC.2012.2196404

EagleView, T. (2014). Pictometry. Retrieved January 01, 2014, from http://www.eagleview.com/Products/ImageSolutionsAnalytics/PictometryImagery.aspx

EEFIT. (2014). The Earthquake Engineering Field Investigation Team. Retrieved November 14, 2014, from http://www.istructe.org/resources-centre/technical-topic-areas/eefit

EMS. (1998). EMS 98. Retrieved January 01, 2014, from http://media.gfz-potsdam.de/gfz/sec26/resources/documents/PDF/EMS-98_Original_englisch.pdf

ESRI. (2014). ArcGIS. Retrieved from http://www.esri.com/software/arcgis

FEMA 306. (1998). *EVALUATION OF EARTHQUAKE DAMAGED CONCRETE AND MASONRY WALL BUILDINGS, Basic Procedures Manual* (p. 247).

FEMA 307. (1998). *EVALUATION OF EARTHQUAKE DAMAGED CONCRETE AND MASONRY WALL BUILDINGS, Technical Resources* (p. 253).

Fritsch, D., & Kilian, J. C. (1994). FILTERING AND CALIBRATION OF LASER SCANNER MEASUREMENTS. In H. Ebner, C. Heipke, & K. Eder (Eds.), *ISPRS Commision I Symposium Munich* (pp. 227–234). Munich. doi:10.1117/12.182831

Galarreta, J. F. (2014). *Urban structural damage assessment using object-oriented analysis and semantic reasoning.* University of Twente, MSc Thesis, Faculty of ITC. Retrieved from http://www.itc.nl/library/papers_2014/msc/aes/fernandez.pdf

Geographics, B. M. (2014). Global Mapper. Retrieved October 05, 2014, from http://www.bluemarblegeo.com/products/global-mapper.php

Georgiou, J. (2010). Verification of a building defect classification system for housing. *Structural Survey*, *28*(5), 370–383. doi:10.1108/02630801011089164

Gerke, M., & Kerle, N. (2011). Automatic Structural Seismic Damage Assessment with Airborne Oblique Pictometry© Imagery. *Photogrammetric Engineering & Remote Sensing*, *77*(9), 885–898. doi:10.14358/PERS.77.9.885

Giakoumis, I., Nikolaidis, N., & Pitas, I. (2006). Digital image procedding techniques for the Detection and Removal of Cracks in Digitized Paintings. In *Image Processing, IEEE* (Vol. 15, pp. 178–188). Retrieved from http://ieeexplore.ieee.org/xpls/abs_all.jsp?arnumber=1556636

Haiyang, Y., Gang, C., & Xiaosan, G. (2010). Earthquake-collapsed building extraction from LiDAR and aerophotograph based on OBIA. In *The 2nd International Conference on Information Science and Engineering* (pp. 2034–2037). IEEE. doi:10.1109/ICISE.2010.5691203

Holland, M. (2012). *Practical Guide to Diagnosing Structural Movement in Buildings* (1st ed., p. 236). Wiley-Blackwell.

Iyer, S., & Sinha, S. K. (2005). A robust approach for automatic detection and segmentation of cracks in underground pipeline images. *Image and Vision Computing*, *23*(10), 921–933. doi:10.1016/j.imavis.2005.05.017

Jahanshahi, M. R., & Masri, S. F. (2012). Adaptive vision-based crack detection using 3D scene reconstruction for condition assessment of structures. *Automation in Construction*, *22*(2), 567–576. doi:10.1016/j.autcon.2011.11.018

Joshi, J. R. (2010). *Improving the quality of digital surface model generated from very high resolution satellite stereo imagery by using Object Oriented Image Analysis technique*. ITC, MSc Thesis, University of Twente.

Kashyzadeh, K., & Kesheh, N. (2012). Study type of Cracks in construction and its controlling. *Citeseer*, *2*(8), 2–5. Retrieved from http://scholar.google.com/scholar?hl=en&btnG=Search&q=intitle:Study+type+of+Cracks+in+construction+and+its+controlling#0

Kerle, N. (2010). Satellite-based damage mapping following the 2006 Indonesia earthquake—How accurate was it? *International Journal of Applied Earth Observation and Geoinformation*, *12*(6), 466–476. doi:10.1016/j.jag.2010.07.004

Kerle, N., & Hoffman, R. R. (2013). Collaborative damage mapping for emergency response: the role of Cognitive Systems Engineering. *Natural Hazards and Earth System Science*, *13*(1), 97–113. doi:10.5194/nhess-13-97-2013

Keshtgar, A., & Modarres, M. (2013). Detecting Crack Initiation Based on Acoustic Emission. *CHEMICAL ENGINEERING*, *33*, 547–552. doi:10.3303/CET1333092

Lemoine, G., Corbane, C., Louvrier, C., & Kauffmann, M. (2013). Intercomparison and validation of building damage assessments based on post-Haiti 2010 earthquake imagery using multi-source reference data. *Natural Hazards and Earth System Sciences Discussions*, *1*(2), 1445–1486. doi:10.5194/nhessd-1-1445-2013

Li, G. (2013). Image-based Method for Concrete Bridge Crack Detection. *Journal of Information and Computational Science*, *10*(8), 2229–2236. doi:10.12733/jics20101784

Li, L. (2012). *Cracks in Different Types of Concrete Construction and Renovation*.

Liu, Z., Suandi, S. A., Ohashi, T., & Ejima, T. (2002). Tunnel crack detection and classification system based on image processing. In M. A. Hunt (Ed.), *Machine Vision Applications in Industrial Inspection* (pp. 145–152). doi:10.1117/12.460191

Marshall, D., Worthing, D., & Heath, R. (2009). *Understanding Housing Defects* (3rd ed., p. 345). Abingdon: Estates Gazette.

Martins, A., Junior Pizolato, J., & Belini, V. (2013). Image-based method for monitoring of crack opening on masonry and concrete using Mobile Platform. *IBRACON*.

Mavrantza, O., & Argialas, D. (2008). An object-oriented image analysis approach for the identification of geologic lineaments in a sedimentary geotectonic environment. *Object-Based Image Analysis*, 383 – 398. Retrieved from http://link.springer.com/chapter/10.1007/978-3-540-77058-9_21

Metni, N., & Hamel, T. (2007). A UAV for bridge inspection: Visual servoing control law with orientation limits. *Automation in Construction*, *17*(1), 3–10. doi:10.1016/j.autcon.2006.12.010

Minehane, M. J., Donovan, R. O., Ruane, K. D., & Keeffe, B. O. (2013). *The Use of 3D Laser Scanning Technology for Bridge Inspection and Assessment* (p. 6).

National Authority on Clay Brick Construction. (2014). Brick Industry Association. Retrieved from http://www.gobrick.com/

Niemeier, W., Riedel, B., Fraser, C., & Neuss, H. (2008). New digital crack monitoring system for measuring and documentation of width of cracks in concrete structures. *FIG/IAG*, *1*, 1–9. Retrieved from http://www.fig.net/commission6/lisbon_2008/papers/pas15/pas15_04_niemeier_mc111.pdf

Nonami, K., Kendoul, F., Suzuki, S., Wang, W., & Nakazawa, D. (2010). *Autonomous Flying Robots*. Tokyo: Springer Japan. doi:10.1007/978-4-431-53856-1

Oh, J.-K., Jang, G., Oh, S., Lee, J. H., Yi, B.-J., Moon, Y. S., … Choi, Y. (2009). Bridge inspection robot system with machine vision. *Automation in Construction*, *18*(7), 929–941. doi:10.1016/j.autcon.2009.04.003

Ohno, K., & Ohtsu, M. (2010). Crack classification in concrete based on acoustic emission. *Construction and Building Materials*, *24*(12), 2339–2346. doi:10.1016/j.conbuildmat.2010.05.004

Pix4D. (2014). Pix4D. Retrieved October 20, 2014, from http://pix4d.com/

R Core Team. (2014). R studio - Manual. Retrieved from http://www.r-project.org/

Riegl. (2014). RIEGL VZ-400. Retrieved from http://www.riegl.com/products/terrestrial-scanning/produktdetail/product/scanner/5/

Riquelme, A., & Abellán, A. (2014). A new approach for semi-automatic rock mass joints recognition from 3D point clouds. *Computers & Geosciences*, *68*, 38–52. doi:10.1016/j.cageo.2014.03.014

Sabnavis, G., Kirk, R. G., Kasarda, M., & Quinn, D. (2004). Cracked Shaft Detection and Diagnostics: A Literature Review. *The Shock and Vibration Digest*, *36*(4), 287–296. doi:10.1177/0583102404045439

Saito, K., & Spence, R. (2010). Damage assessment of Port-au-Prince using Pictometry. *Proceedings of the …*, (October). Retrieved from http://www.enveng.titech.ac.jp/midorikawa/rsdm2010_pdf/18_saito_paper.pdf

Santhi, B., Krishnamurthy, G., Siddharth, S., & Ramakrishnan, P. K. (2012). AUTOMATIC DETECTION OF CRACKS IN PAVEMENTS USING EDGE DETECTION OPERATOR. *Journal of Theoretical and Applied Information Technology*, *36*(2), 199–205.

SKEYE BV. (2014). Skeye. Retrieved from http://www.skeyebv.com/

Sohn, H., & Lim, Y. (2005). Monitoring crack changes in concrete structures. *Computer-Aided Civil and …*, *20*(1), 52–61. doi:10.1111/j.1467-8667.2005.00376.x

Stanford University. (2014). Building Assessment Team (BAT). *BAT*. Retrieved November 13, 2014, from http://web.stanford.edu/dept/EHS/prod/general/erprep/bat.html

Stumpf, A., Malet, J.-P., Kerle, N., Niethammer, U., & Rothmund, S. (2013). Image-based mapping of surface fissures for the investigation of landslide dynamics. *Geomorphology*, *186*, 12–27. doi:10.1016/j.geomorph.2012.12.010

Tian, Y., & Zhang, J. (2004). Techniques for seismic damages assessment by using remotely sensed images. *… 2004. IGARSS'04. Proceedings. 2004 IEEE …*, *00*(Icd), 1422–1425. Retrieved from http://ieeexplore.ieee.org/xpls/abs_all.jsp?arnumber=1368686

Torok, M., Fard, M. G., & Kochersberger, K. B. (2012). Post-Disaster Robotic Building Assessment: Automated 3D Crack Detection from Image-Based Reconstructions. In *Computing in Civil Engineering (2012)* (pp. 397–404). Reston, VA: American Society of Civil Engineers. doi:10.1061/9780784412343.0050

Torok, M., Golparvar-Fard, M., & Kochersberger, K. (2014). Image-Based Automated 3D Crack Detection for Post-disaster Building Assessment. *Journal of Computing in Civil Engineering*, *28*(5), A4014004. doi:10.1061/(ASCE)CP.1943-5487.0000334

Trimble. (2014a). eCognition. Trimble Developper. Retrieved August 15, 2014, from http://www.trimble.com/

Trimble. (2014b). *eCognition User Guide* (p. 25). Retrieved from http://www.ecognition.com/

Tsao, S., Kehtarnavaz, N., Chan, P., & Lytton, R. (1994). Image-Based Expert-System approach to distress detection on CRC pavement. *Journal of Transportation Engineering*, *120*(1), 52–64. doi:10.1061/(ASCE)0733-947X(1994)120:1(52)

UNITAR. (2014). United Nations Institute for Training and Research: Operational Satellite Applications Programme. Retrieved November 10, 2014, from http://www.unitar.org/unosat/

Valença, J., Dias-da-Costa, D., & Júlio, E. N. B. S. (2012). Characterisation of concrete cracking during laboratorial tests using image processing. *Construction and Building Materials*, *28*(1), 607–615. doi:10.1016/j.conbuildmat.2011.08.082

Yamaguchi, T., & Hashimoto, S. (2009). Fast crack detection method for large-size concrete surface images using percolation-based image processing. *Machine Vision and Applications*, *21*(5), 797–809. doi:10.1007/s00138-009-0189-8

Yamazaki, F., Suzuki, D., & Maruyama, Y. (2008). Detection of damages due to earthquakes using digital aerial images. *Proceedings of 6th International …, 2007*. Retrieved from http://tlc.unipv.it/6_RSDMA/Finals/1.4 - Yamazaki_ppt.pdf

Yu, S., Jang, J., & Han, C. (2007). Auto inspection system using a mobile robot for detecting concrete cracks in a tunnel. *Automation in Construction*, *16*(3), 255–261. doi:10.1016/j.autcon.2006.05.003

Zhang, Y., & Kerle, N. (2008). Satellite remote sensing for near-real time data collection (p. 75). Taylor & Francis Group.

Zhu, Z., German, S., & Brilakis, I. (2011). Visual retrieval of concrete crack properties for automated post-earthquake structural safety evaluation. *Automation in Construction*, *20*(7), 874–883. doi:10.1016/j.autcon.2011.03.004

7. APPENDIX

7.1. Orthophoto inventory

Concrete sample I	
Flash	No Flash
	
Concrete sample II	
Flash	No Flash
	
Brick sample I	
Flash	No Flash
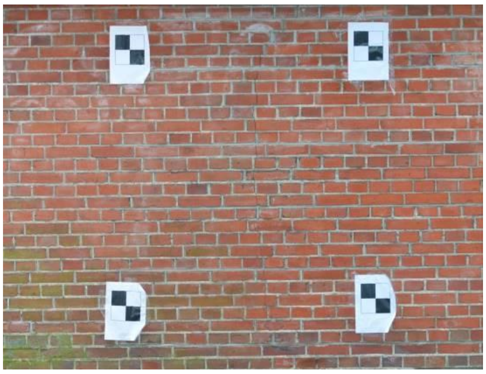	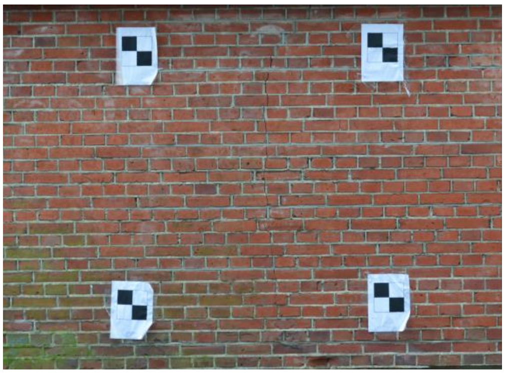

Brick sample II	
Flash	No Flash
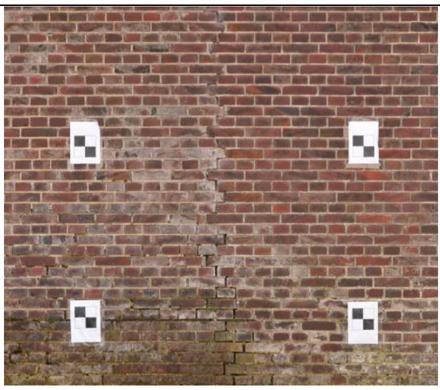	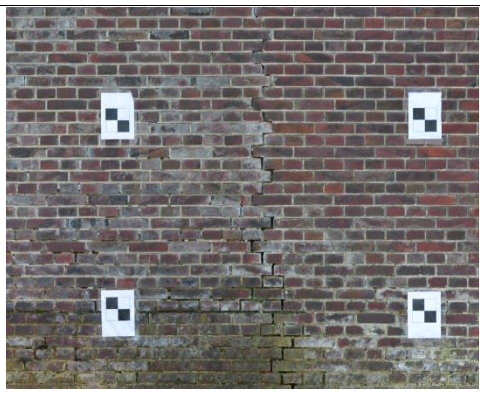
ITC insulating sampling	
Flash	No Flash
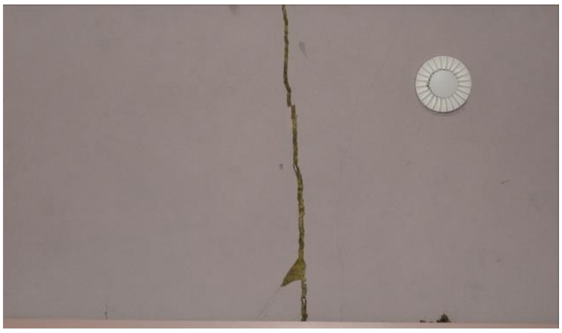	

7.2. DSM inventory

<table>
<tr><td colspan="2">Concrete sample I</td></tr>
<tr><td>Flash</td><td>No Flash</td></tr>
<tr><td>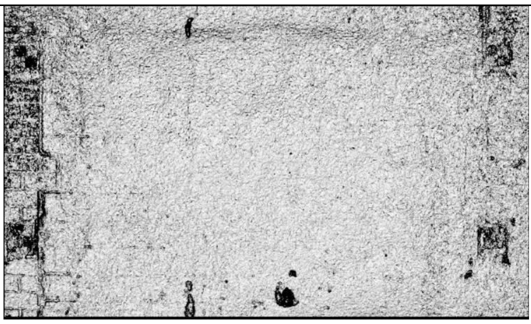</td><td>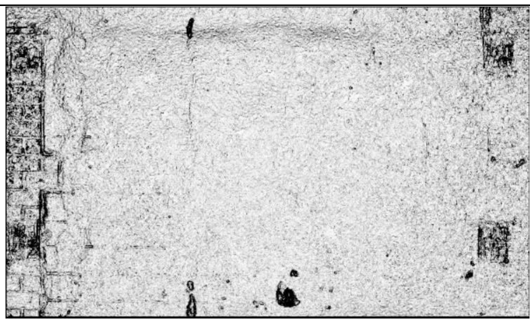</td></tr>
<tr><td colspan="2">Concrete sample II</td></tr>
<tr><td>Flash</td><td>No Flash</td></tr>
<tr><td>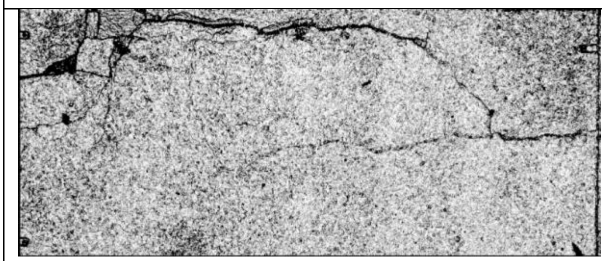</td><td></td></tr>
<tr><td colspan="2">Brick sample I</td></tr>
<tr><td>Flash</td><td>No Flash</td></tr>
<tr><td>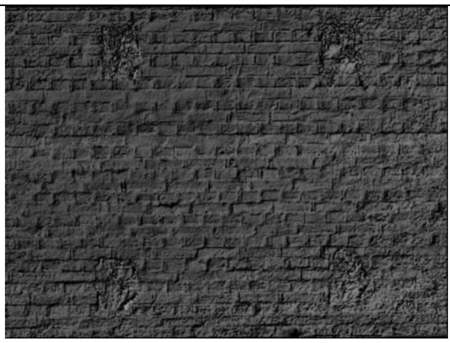</td><td>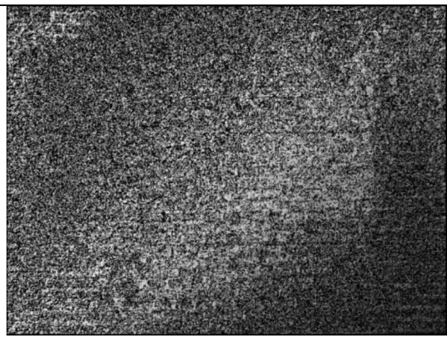</td></tr>
<tr><td colspan="2"></td></tr>
</table>

Brick sample II	
Flash	No Flash
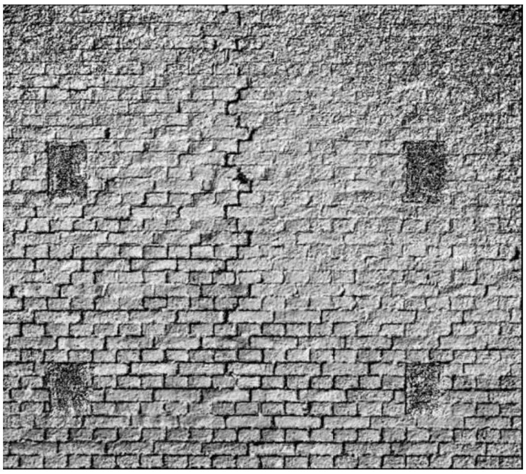	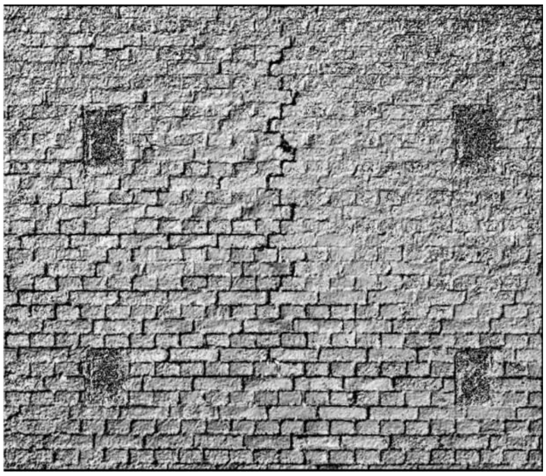
ITC insulating sampling	
Flash	No Flash
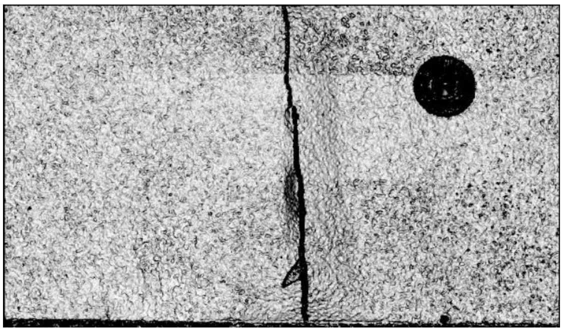	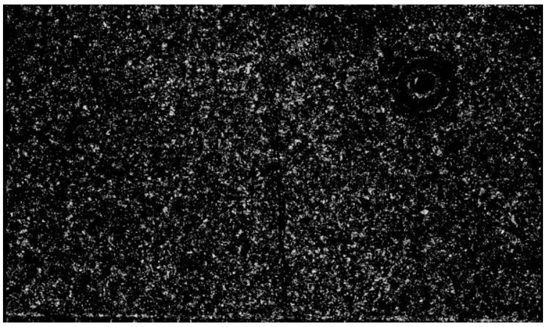

7.3. R environment

```
require(rgdal)
require(rgeos)
require(maptools)

# A. Read reference
x = readOGR("C:/Test/itc/Reference", "itc_noflash")
areax = gArea(x, byid=TRUE) #calculates the area of the given geometry   - SAVE in txt
write.table(areax,"C:/Test/itc/Reference/nameoftxt")

# A1. Buffer of reference
buffx = gBuffer(x, byid=FALSE, id=NULL, width=0.05, quadsegs=5, capStyle="ROUND",
joinStyle="ROUND", mitreLimit=1.0)#Generates a buffer at given width
areaBuffx = gArea(buffx, byid=FALSE)#calculates the area of the reference buffer
write.table(areaBuffx,"C:/Test/itc/OBIA/areaBuffx")

# A2. Envelope of buffer of reference
envx = gEnvelope(buffx, byid=TRUE, id = NULL) #the minimum bounding box is created

# A3. Plot of reference items
windows()
plot(envx, border='green')
plot(buffx, add=TRUE, col='yellow')
plot(x, add=TRUE, col='green')

# B. Read OBIA
y = readOGR("C:/Test/itc/OBIA", "ITC_NOFLASH.v1")
areay = gArea(y, byid=TRUE) #calculates the area of the OBIA geometry   - SAVE in txt
write.table(areay,"C:/Test/itc/OBIA/areay")

# B1. Envelope of OBIA
envy = gEnvelope(y, byid=TRUE, id = NULL) #the minimum bounding box is created

# B2. Plot of OBIA items
windows()
plot(envy,border='blue')
plot(y, add=TRUE, col='blue')
```

```
##############################
###        Comparison              #####
##############################

# Compare OBIA with buffer from reference
diff = gIntersection(y, buffx, byid = TRUE)
str(diff)

windows()
plot(diff, col='red')
plot(buffx, add=TRUE, col='green')
plot(y, add=TRUE, col='blue')
areadiff = gArea(diff, byid=TRUE)
write.table(areadiff,"C:/Test/itc/OBIA/areadiff")

Percentage = areadiff/areaBuffx
write.table(Percentage,"C:/Test/itc/OBIA/PercentageITC_NOFLASH")
```

7.4. OBIA rulesets

7.4.1. Galarreta's rulesets

"concrete" ruleset

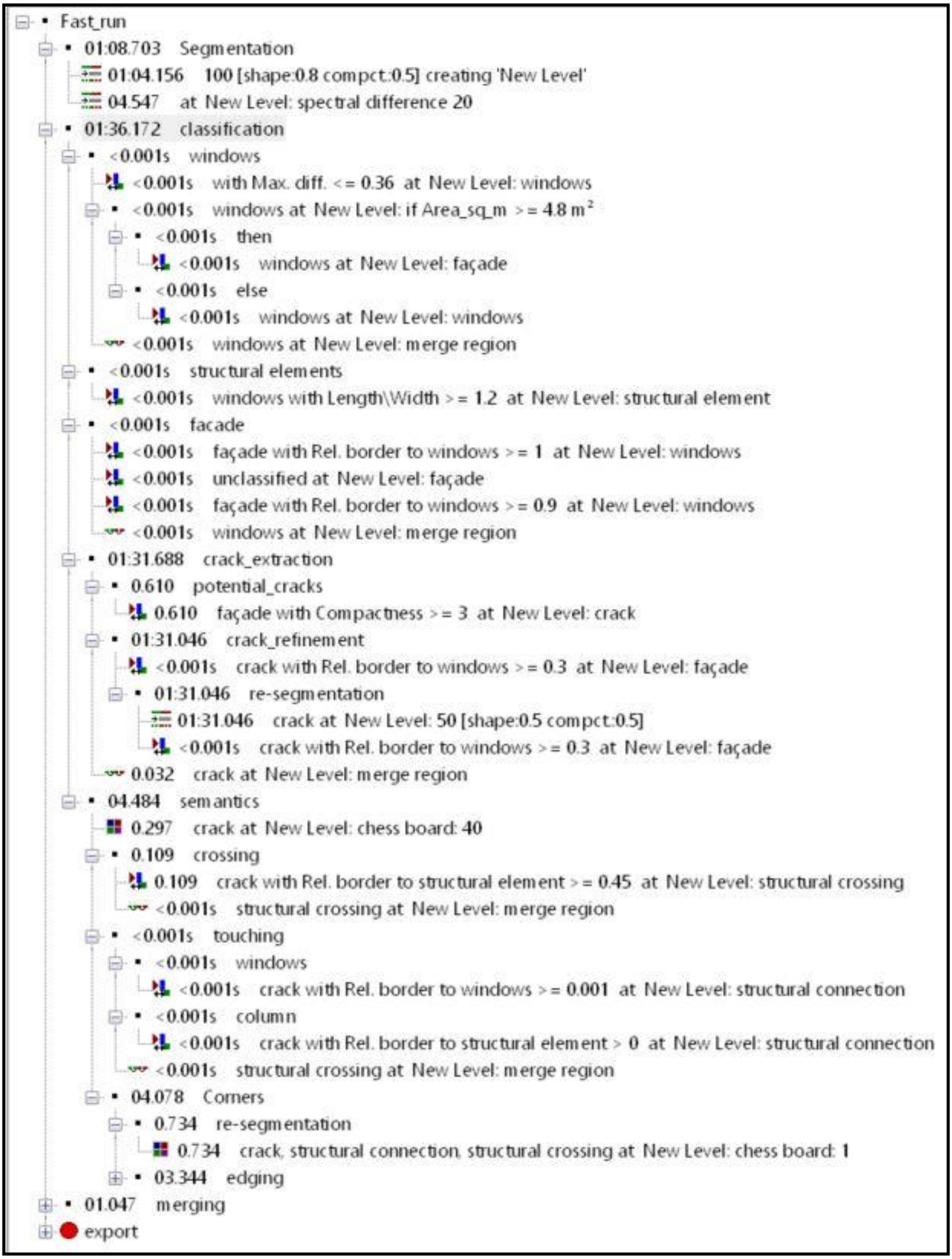

```
Fast_run
  01:08.703  Segmentation
    01:04.156  100 [shape:0.8 compct:0.5] creating 'New Level'
    04.547  at New Level: spectral difference 20
  01:36.172  classification
    <0.001s  windows
      <0.001s  with Max. diff. <= 0.36 at New Level: windows
      <0.001s  windows at New Level: if Area_sq_m >= 4.8 m²
        <0.001s  then
          <0.001s  windows at New Level: façade
        <0.001s  else
          <0.001s  windows at New Level: windows
      <0.001s  windows at New Level: merge region
    <0.001s  structural elements
      <0.001s  windows with Length\Width >= 1.2 at New Level: structural element
    <0.001s  facade
      <0.001s  façade with Rel. border to windows >= 1 at New Level: windows
      <0.001s  unclassified at New Level: façade
      <0.001s  façade with Rel. border to windows >= 0.9 at New Level: windows
      <0.001s  windows at New Level: merge region
    01:31.688  crack_extraction
      0.610  potential_cracks
        0.610  façade with Compactness >= 3 at New Level: crack
      01:31.046  crack_refinement
        <0.001s  crack with Rel. border to windows >= 0.3 at New Level: façade
        01:31.046  re-segmentation
          01:31.046  crack at New Level: 50 [shape:0.5 compct:0.5]
          <0.001s  crack with Rel. border to windows >= 0.3 at New Level: façade
      0.032  crack at New Level: merge region
    04.484  semantics
      0.297  crack at New Level: chess board: 40
      0.109  crossing
        0.109  crack with Rel. border to structural element >= 0.45 at New Level: structural crossing
        <0.001s  structural crossing at New Level: merge region
      <0.001s  touching
        <0.001s  windows
          <0.001s  crack with Rel. border to windows >= 0.001 at New Level: structural connection
        <0.001s  column
          <0.001s  crack with Rel. border to structural element > 0 at New Level: structural connection
        <0.001s  structural crossing at New Level: merge region
      04.078  Corners
        0.734  re-segmentation
          0.734  crack, structural connection, structural crossing at New Level: chess board: 1
        03.344  edging
  01.047  merging
  export
```

Galarreta “brick” ruleset

- fast_run
  - segmentation
    - 25 [shape:0.2 compct:0.2] creating 'New Level'
    - at New Level: spectral difference 35
  - binary_class
    - with Area_sq_m >= 3 m^2 at New Level: Facade
    - unclassified at New Level: damage
    - damage_refinement
      - refinement of the damage feature
      - damage with Rectangular Fit >= 0.87 and Area_sq_m <= 0.05 m^2 at New Level: Facade
      - damage with Max. diff. >= 0.33 and Max. diff. <= 0.35 at New Level: Facade
  - Features_classification
    - damage with Area_sq_m >= 0.05 m^2 and Asymmetry <= 0.61 at New Level: hole
    - damage at New Level: crack
    - Facade, unclassified at New Level: merge region
    - crack at New Level: merge region
    - hole at New Level: merge region
    - hole with Rectangular Fit >= 0.85 and Area_sq_m <= 1.2 m^2 at New Level: window
    - cracks_refinement
      - crack with Length\Width >= 5.6 at New Level: Facade
      - crack with Area_sq_m <= 0.002 m^2 at New Level: Facade
  - semantics
    - connection
      - windows
        - crack with Rel. border to window >= 0.001 at New Level: structural_touching
      - holes
        - crack with Rel. border to hole > 0 at New Level: structural_touching
  - aggregation
    - Column at New Level: merge region
    - crack at New Level: merge region
    - structural crossing at New Level: merge region
    - structural_touching at New Level: merge region
    - Facade at New Level: merge region
    - window at New Level: merge region
  - at New Level: export object shapes to ObjectShapes

7.4.2. Developed rulesets

“Concrete” ruleset

- Concrete
  - Segmentation
    - 90 [shape:0.2 compct.:0.2] creating 'New Level'
    - at New Level: spectral difference 10
  - Binary
    - with Brightness <= 338 and Mean DSM <= 1000.4 at New Level: Damage
    - unclassified at New Level: Facade
    - Facade at New Level: merge region
    - Damage at New Level: merge region
  - Facade refinement
    - Damage with Area >= 35000 Pxl or Area <= 4000 Pxl at New Level: Facade
    - Facade at New Level: merge region
  - Classification
    - Damage at New Level: Hole
    - Damage with Length\Width >= 3 and Asymmetry >= 0.9 at New Level: Crack
    - Crack at New Level: merge region
    - Hole at New Level: merge region
  - export
    - Crack, Hole at New Level: export object shapes to ObjectShapes

Updated ruleset for “Concrete II”

- Concrete
  - Segmentation
    - 90 [shape:0.2 compct.:0.2] creating 'New Level'
    - at New Level: spectral difference 10
  - Binary
    - with Brightness <= 291 and Mean DSM <= 1000 at New Level: Damage
    - unclassified at New Level: Facade
    - Facade at New Level: merge region
    - Damage at New Level: merge region
  - Facade refinement
    - Damage with Area >= 35000 Pxl or Area <= 1200 Pxl at New Level: Facade
    - Facade at New Level: merge region
  - Classification
    - Damage at New Level: Hole
    - Damage with Length\Width >= 3 and Asymmetry >= 0.9 at New Level: Crack
    - Crack at New Level: merge region
    - Hole at New Level: merge region
  - export
    - Crack, Hole at New Level: export object shapes to ObjectShapes

“Brick” ruleset

- Brick
  - Segmentation
    - 25 [shape:0.2 compct.:0.2] creating 'New Level'
    - at New Level: spectral difference 15
  - Binary
    - with Brightness <= 299 and Mean DSM <= 999 at New Level: Damage
    - Damage with Area <= 470 Pxl at New Level: Facade
    - unclassified at New Level: Facade
    - Facade at New Level: merge region
  - Classification
    - Damage at New Level: Crack
    - Crack at New Level: merge region
    - with Area <= 2500 Pxl at New Level: Hole
    - Hole at New Level: merge region
  - export
    - Crack, Hole at New Level: export object shapes to ObjectShapes

Updated ruleset for “Brick I”

Flash sample

- Brick
  - Segmentation
    - 25 [shape:0.2 compct.:0.2] creating 'New Level'
    - at New Level: spectral difference 15
  - Binary
    - with Brightness <= 310 and Mean DSM <= 1001 at New Level: Damage
    - Damage with Area <= 250 Pxl or Area >= 250000 Pxl at New Level: Facade
    - unclassified at New Level: Facade
    - Facade at New Level: merge region
  - Classification
    - Damage at New Level: Hole
    - Damage with Length\Width >= 5 at New Level: Crack
    - Crack at New Level: merge region
    - Hole at New Level: merge region
  - export
    - Crack, Hole at New Level: export object shapes to ObjectShapes

Updated ruleset for “Brick I”

No flash sample

- Brick
  - Segmentation
    - 25 [shape:0.2 compct.:0.2] creating 'New Level'
    - at New Level: spectral difference 15
  - Binary
    - with Brightness <= 323 and Mean DSM <= 999.8 at New Level: Damage
    - Damage with Area <= 250 Pxl at New Level: Facade
    - unclassified at New Level: Facade
    - Facade at New Level: merge region
  - Classification
    - Damage at New Level: Hole
    - Damage, Hole with Length\Width >= 2.5 at New Level: Crack
    - Crack at New Level: merge region
    - Hole at New Level: merge region
  - export
    - Crack, Hole at New Level: export object shapes to ObjectShapes

“Insulating” ruleset

- ITC_material
- Segmentation
  - 100 [shape:0.8 compct.:0.5] creating 'New Level'
  - at New Level: spectral difference 20
- Binary
  - with Brightness <= 310 and Area <= 55000 Pxl and Mean DSM <= 1000.3 at New Level: Damage
  - unclassified at New Level: Facade
  - Facade at New Level: merge region
- Feature selection
  - Damage with Rectangular Fit >= 0.5 and Length\Width <= 5 at New Level: Hole
  - Damage with Length\Width >= 5 at New Level: Crack
- <0.001s Export
  - at New Level: export object shapes to ObjectShapes

7.5. Accuracy assessment

“Concrete I” no flash

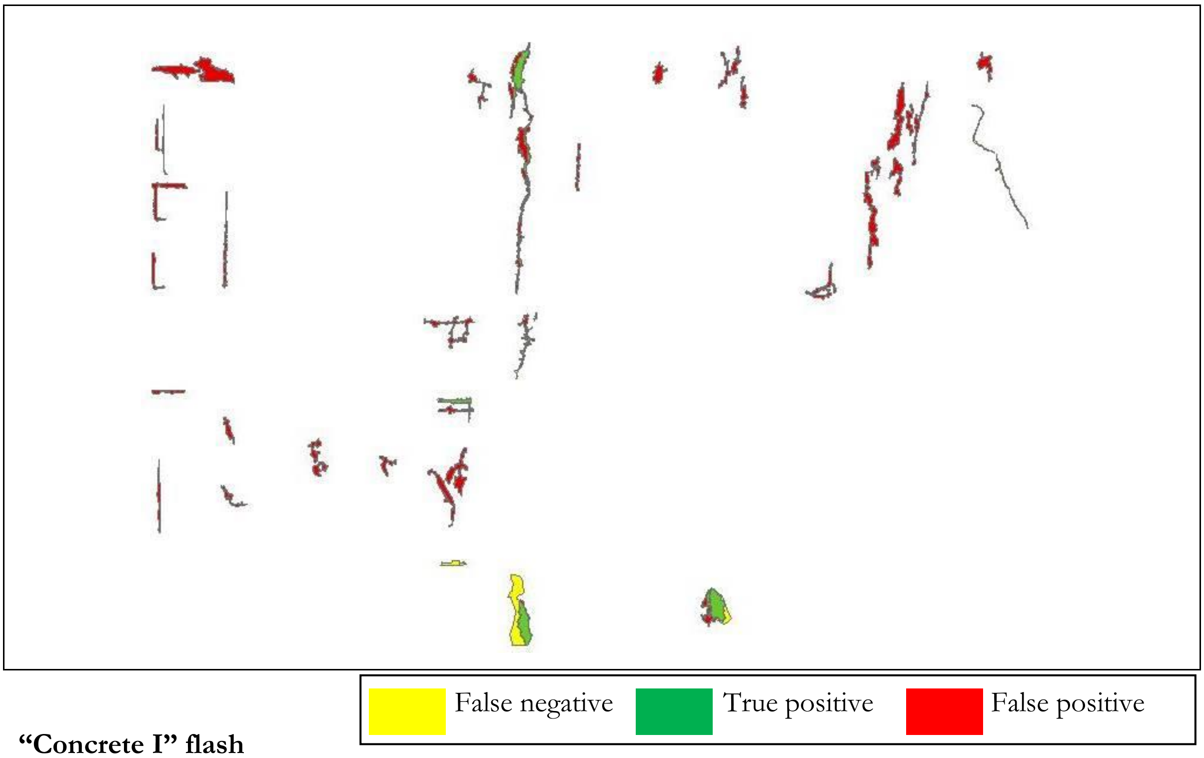

“Concrete I” flash

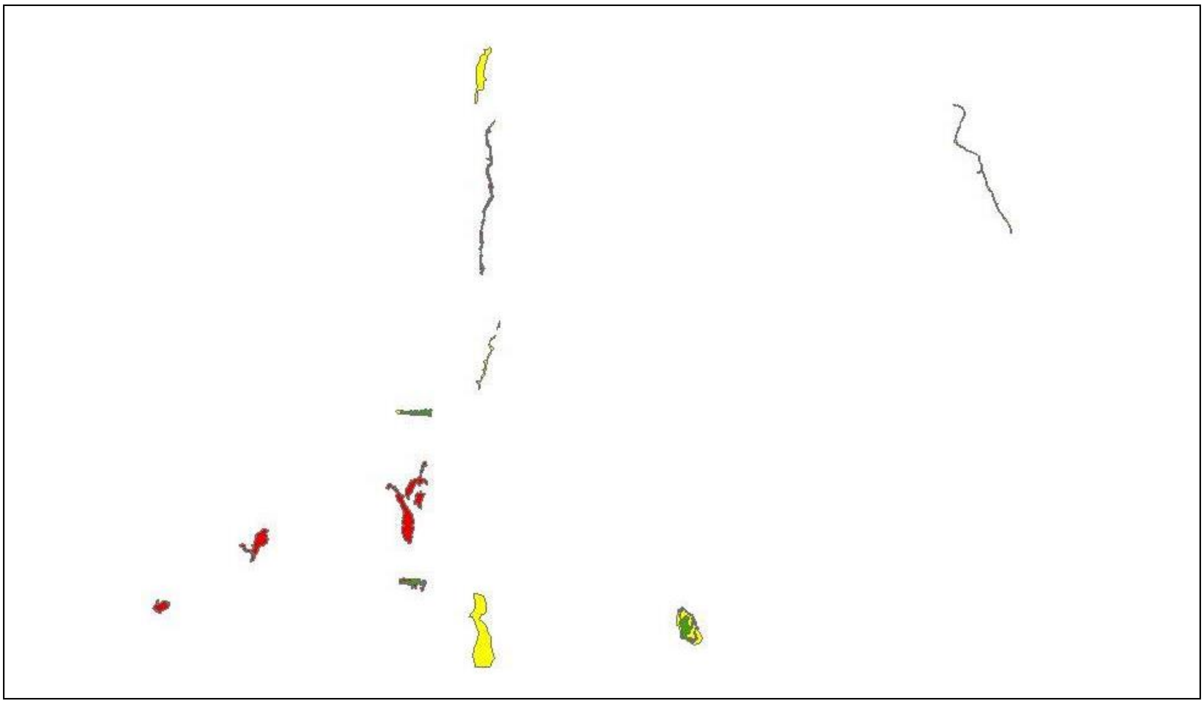

Illustration of the results of the accuracy assessment (Concrete I flash & no flash)

"Concrete II" no flash

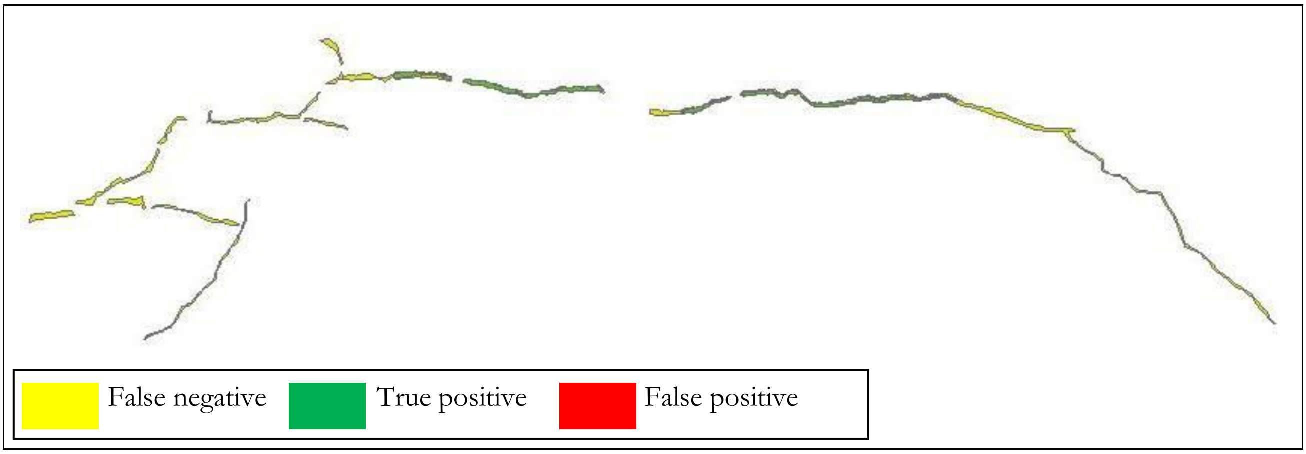

"Concrete II" flash

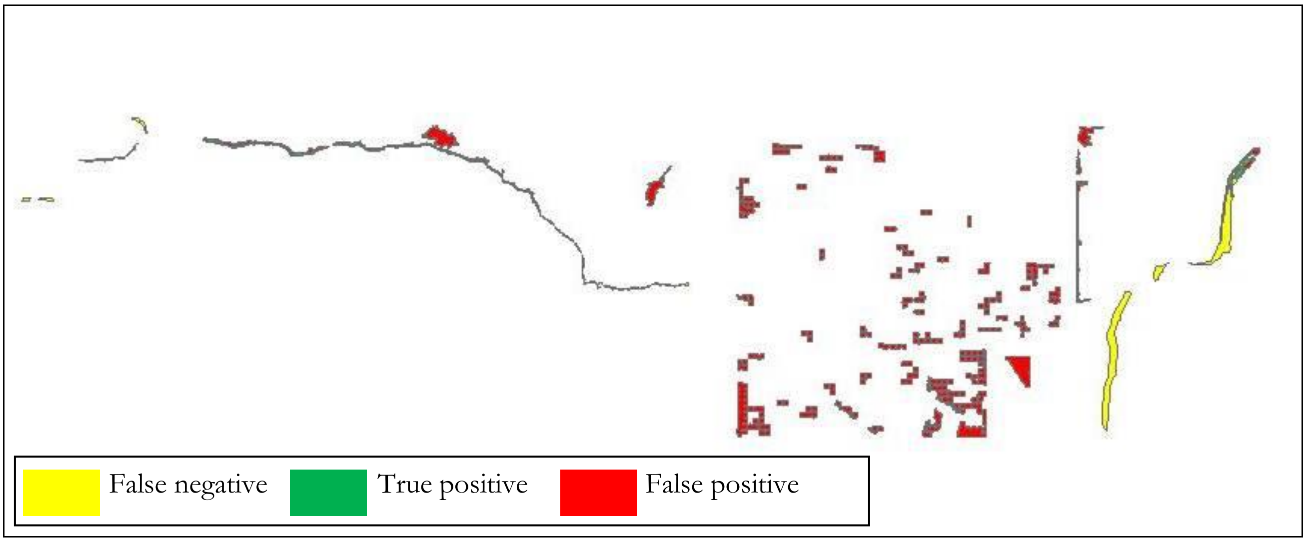

Illustration of the results of the accuracy assessment (Concrete II flash & no flash)

“Brick I” no flash

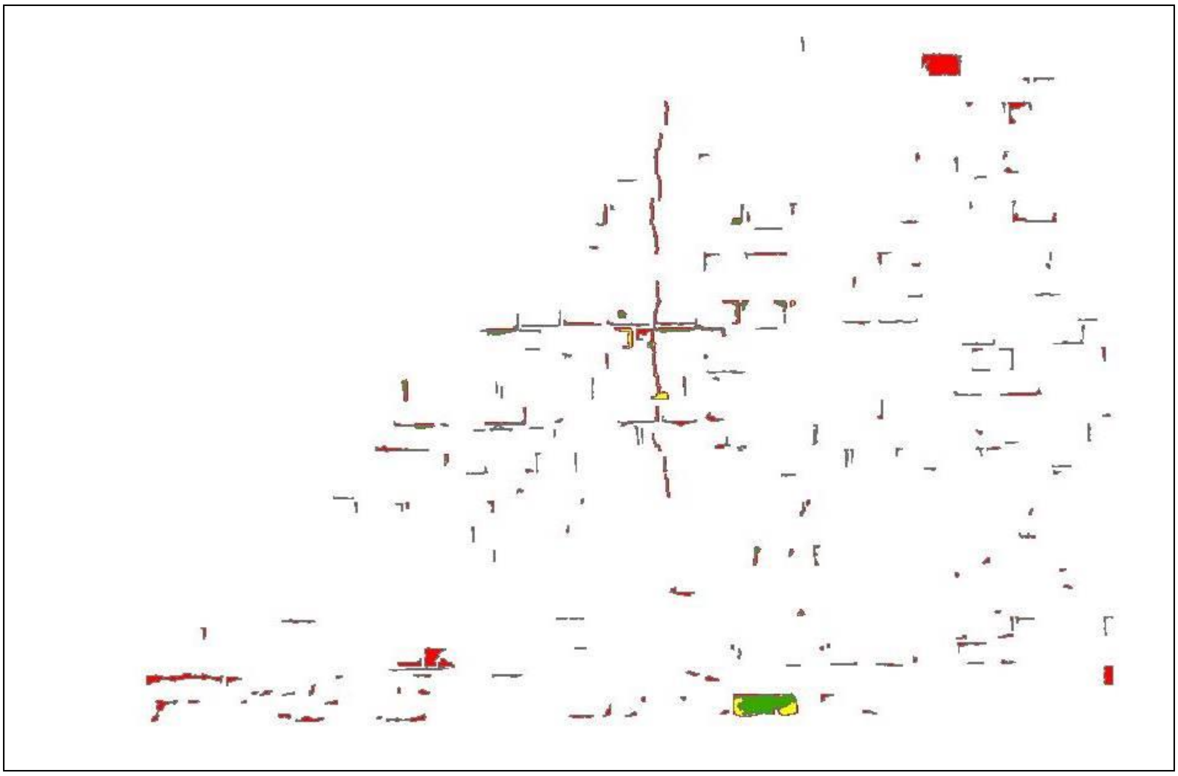

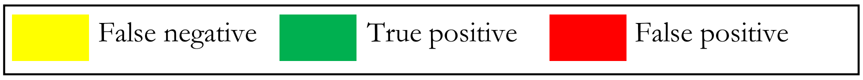

“Brick I” flash

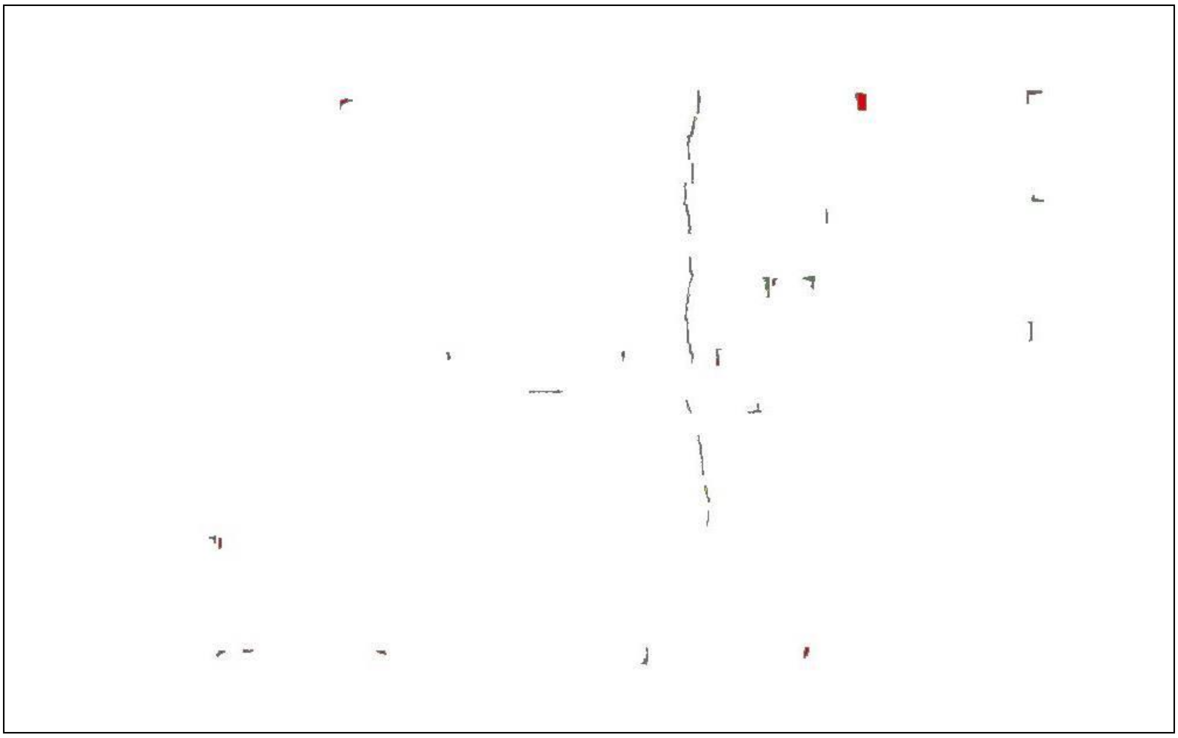

Illustration of the results of the accuracy assessment (Brick I flash & no flash)

“Brick II” no flash

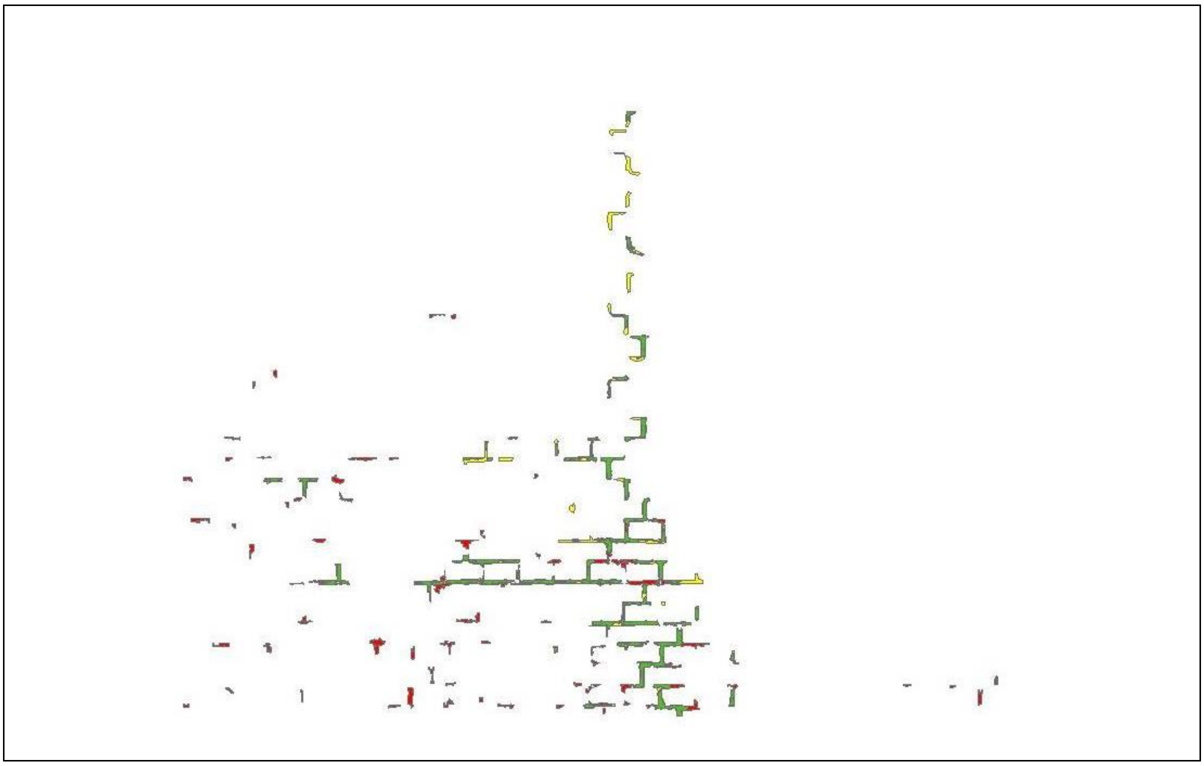

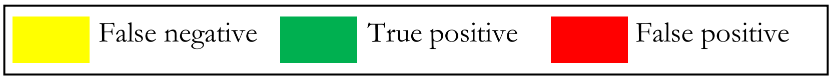

“Brick II” flash

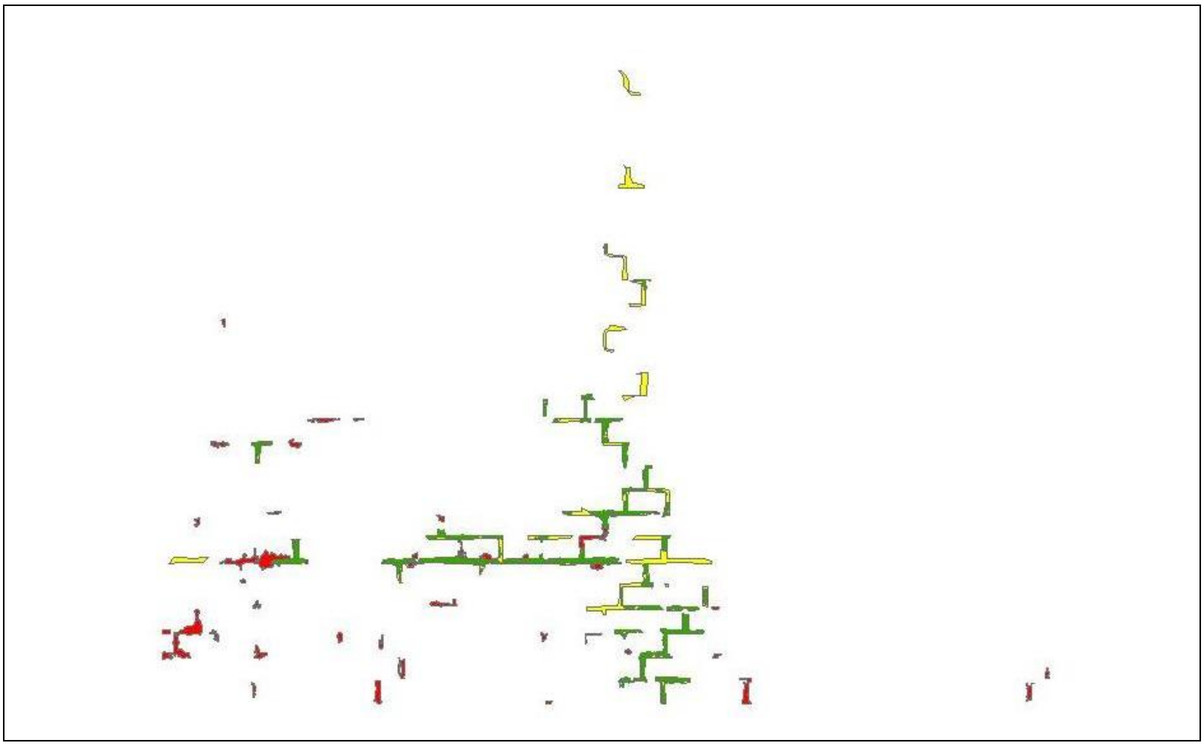

Illustration of the results of the accuracy assessment (Brick II flash & no flash)

“Insulating material” no flash

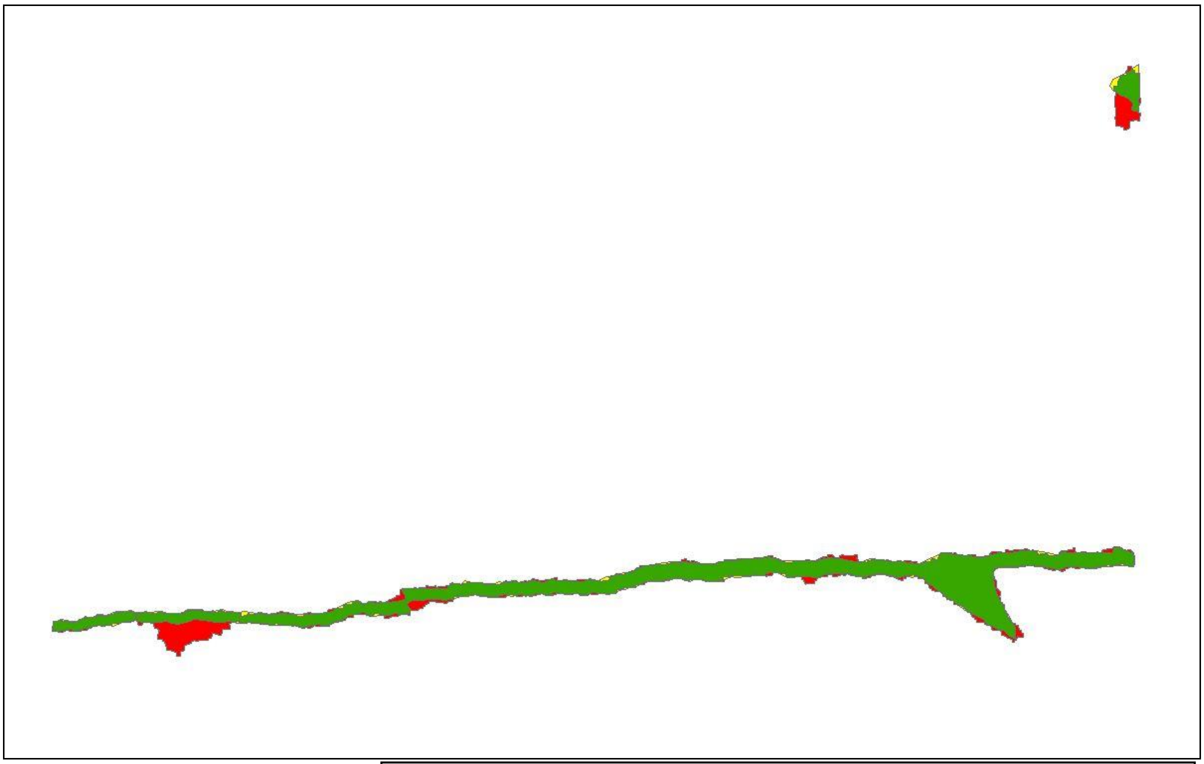

“Insulating material” flash

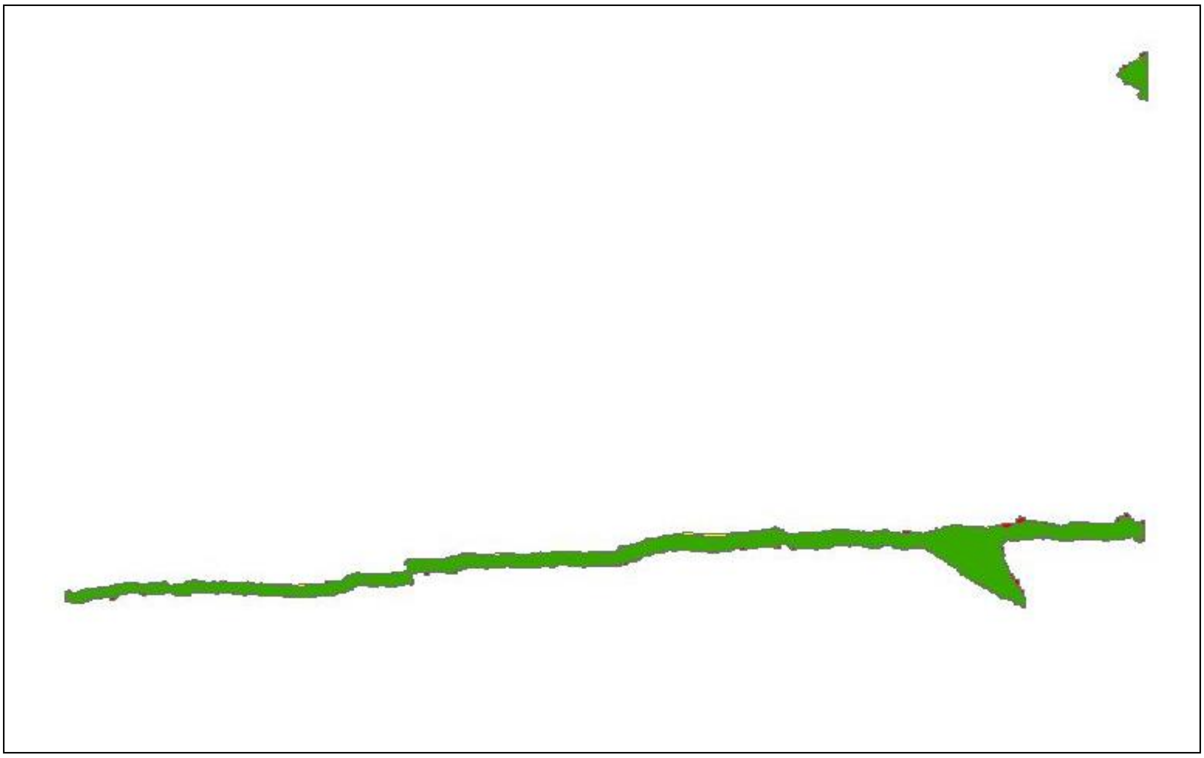

Illustration of the results of the accuracy assessment (Insulating material flash & no flash)

7.6. Point cloud registration